The Nordic Seas carbon budget: Sources, sinks, and uncertainties

Emil Jeansson,[1,2] Are Olsen,[1,2,3] Tor Eldevik,[4,5] Ingunn Skjelvan,[1,2,4]
Abdirahman M. Omar,[1,2] Siv K. Lauvset,[4,5] Jan Even Ø. Nilsen,[6]
Richard G. J. Bellerby,[1,2,4] Truls Johannessen,[4,5,7] and Eva Falck[1,2,8]

Received 22 September 2010; revised 8 June 2011; accepted 16 September 2011; published 9 December 2011.

[1] A carbon budget for the Nordic Seas is derived by combining recent inorganic carbon data from the CARINA database with relevant volume transports. Values of organic carbon in the Nordic Seas' water masses, the amount of carbon input from river runoff, and the removal through sediment burial are taken from the literature. The largest source of carbon to the Nordic Seas is the Atlantic Water that enters the area across the Greenland-Scotland Ridge; this is in particular true for the anthropogenic CO_2. The dense overflows into the deep North Atlantic are the main sinks of carbon from the Nordic Seas. The budget show that presently 12.3 ± 1.4 Gt C yr^{-1} is transported into the Nordic Seas and that 12.5 ± 0.9 Gt C yr^{-1} is transported out, resulting in a net advective carbon transport out of the Nordic Seas of 0.17 ± 0.06 Gt C yr^{-1}. Taking storage into account, this implies a net air-to-sea CO_2 transfer of 0.19 ± 0.06 Gt C yr^{-1} into the Nordic Seas. The horizontal transport of carbon through the Nordic Seas is thus approximately two orders of magnitude larger than the CO_2 uptake from the atmosphere. No difference in CO_2 uptake was found between 2002 and the preindustrial period, but the net advective export of carbon from the Nordic Seas is smaller at present due to the accumulation of anthropogenic CO_2.

Citation: Jeansson, E., A. Olsen, T. Eldevik, I. Skjelvan, A. M. Omar, S. K. Lauvset, J. E. Ø. Nilsen, R. G. J. Bellerby, T. Johannessen, and E. Falck (2011), The Nordic Seas carbon budget: Sources, sinks, and uncertainties, *Global Biogeochem. Cycles*, *25*, GB4010, doi:10.1029/2010GB003961.

1. Introduction

[2] Identifying sources and sinks of carbon in the ocean, and their temporal and spatial variability, is vital to understanding the past, present, and future oceanic carbon system. Key questions are: How does the system respond to changes in climate, and to the increasing load of CO_2 in the atmosphere? The carbon cycle of the preindustrial times is understood to have been in balance and thus operated in steady state [e.g., *Sarmiento et al.*, 2000]. However, because of the anthropogenic CO_2 (C_{ant}) released to the atmosphere since the industrial revolution [*Sabine et al.*, 2004], the present carbon system is not in steady state. The oceans have taken up about half of the C_{ant} emitted from the burning of fossil fuels [*Sabine et al.,* 2004], and changes in the net uptake can have a large effect on future global climate change as projected by earth system models [e.g., *Sarmiento and Gruber*, 2002]. There is evidence of a reduced North Atlantic CO_2 uptake during the last decade [*Schuster et al.*, 2009], however, the interannual variability in the North Atlantic CO_2 uptake is large [e.g., *Watson et al.,* 2009] and is probably affected by regional ocean-atmosphere variability such as the North Atlantic Oscillation (NAO) [e.g., *Gruber et al.*, 2002; *Thomas et al.,* 2008; *Herbaut and Houssais*, 2009; *Ullman et al.,* 2009].

[3] The Nordic Seas (the collective term for the Greenland, Iceland and Norwegian Seas) host the northern limb of the Atlantic Ocean's thermohaline circulation (THC) and are the North Atlantic Ocean's gateway to the Arctic Ocean. Some of the world's densest waters are formed at the source of the THC's northern overturning. This ventilation transports carbon from the surface layer to the intermediate and deep waters of the ocean. Thus the Nordic Seas acts as a channel for atmospheric CO_2 from surface to depth, a process that sustains the global ocean carbon sink [e.g., *Sabine et al.,* 2004]. *Olsen et al.* [2010] recently estimated the inventory of C_{ant} in the Nordic Seas to be in the range 0.9–1.4 Gt C (1 Gt = 10^{15} g), which is approximately 1% of the global ocean C_{ant} inventory [*Sabine et al.,* 2004]. Considering that the Nordic Seas only comprise ~0.3% of the global ocean volume, the area stores a relatively large amount of C_{ant}.

[4] In this study we evaluate present (2002) and preindustrial carbon transport through the gateways connecting the Nordic Seas with the North Atlantic and the Arctic Ocean. The only published carbon budget of the Nordic Seas

[1]Uni Bjerknes Centre, Uni Research AS, Bergen, Norway.
[2]Bjerknes Centre for Climate Research, Bergen, Norway.
[3]Now at Institute for Marine Research, Bergen, Norway.
[4]Geophysical Institute, University of Bergen, Bergen, Norway.
[5]Also at Bjerknes Centre for Climate Research, Bergen, Norway.
[6]Nansen Environmental and Remote Sensing Centre, Bergen, Norway.
[7]Also at Uni Bjerknes Centre, Uni Research AS, Bergen, Norway.
[8]Now at Geophysical Institute, University of Bergen, Bergen, Norway.

0886-6236/11/2010GB003961

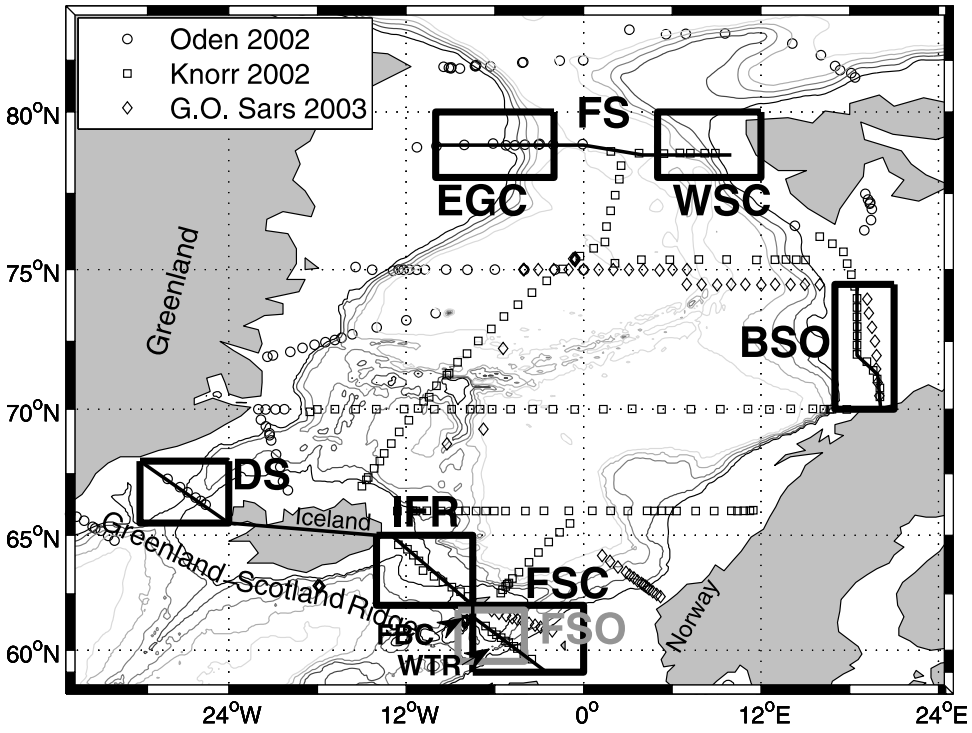

Figure 1. Map showing the stations of the CARINA data used in the budget. The boxes define the boundaries used for the different gateways in the budget. Abbreviations: BSO, Barents Sea Opening; DS, Denmark Strait; EGC, East Greenland Current; FBC, Faroe Bank Channel; FS, Fram Strait; FSC, Faroe-Shetland Channel; FSO, Faroe-Shetland overflow; IFR, Iceland-Faroe Ridge; WSC, West Spitsbergen Current; WTR, Wyville-Thomson Ridge. Solid black lines indicate the sections plotted in Figures 2–4.

to date is by *Lundberg and Haugan* [1996] (also including the Arctic Ocean), using data from only a few stations sampled in the early 1980s. Since then there have been great improvements in data coverage and measurement techniques. This has resulted in increased knowledge both of the physical system [*Rudels et al.*, 1999; *Hansen and Østerhus,* 2000; *Blindheim and Rey*, 2004] and of the Nordic Seas' carbon system [*Skjelvan et al.*, 2005; *Olsen et al.*, 2006]. Our study takes advantage of the recent progress, in particular the new and comprehensive observational database CARINA [*Key et al.,* 2010], which has excellent coverage in the Nordic Seas [*Olsen,* 2009a, 2009b; *Olsen et al.,* 2009; *Jeansson et al.*, 2010]. We compile an up-to-date carbon budget for the Nordic Seas, including uncertainties, by combining the observed carbon concentrations of the water masses exchanged through the gateways with the associated volume transports. The most important pathways of carbon are thus identified and, together with an estimate of the storage, the Nordic Seas' uptake of atmospheric CO_2 is quantified accordingly.

2. Brief Description of the Nordic Seas

[5] The Nordic Seas are separated from the North Atlantic in the south by the Greenland-Scotland Ridge (GSR) and from the Arctic Ocean by the shallow Barents Sea in the northeast and the 2600 m deep Fram Strait to the north (Figure 1). The main inflow to the area occurs in the south as warm and salty Atlantic Water (AW) carried within the Norwegian Atlantic Current, in the north as cold and relatively fresh Polar Water (PW) and as denser waters within the East Greenland Current (EGC). The southern outflow across the GSR consists of PW in the surface and dense overflow waters formed within the Nordic Seas and the Arctic Ocean, at depth. The mean depth of the ridge (~500 m) limits the exchange of deep water with the North Atlantic and the only regions that allow relatively deep overflows are the Denmark Strait (~650 m) and the Faroe Bank Channel (~850 m), but shallower overflow also occurs across the Iceland-Faroe Ridge and the Wyville-Thomson Ridge [e.g., *Hansen and Østerhus*, 2000] (Figure 1). Outflow of AW to the Arctic Ocean occurs via the shallow Barents Sea and within the West Spitsbergen Current (WSC) through the Fram Strait. In the Fram Strait there is also a rather large exchange of deep water [e.g., *Schauer et al.*, 2004]. The Nordic Seas are also connected to the North Sea in the southeast, where the Norwegian Coastal Current (NCC) brings in relatively fresh water, originating in the Skagerrak and the Baltic Sea [*Gammelsrød and Hackett*, 1981; *Björk et al.*, 2001]. The NCC flows northward along the Norwegian coast and exits the Nordic Seas through the Barents Sea Opening.

3. Data

[6] The data used for the budget are taken from the database CARbon IN the Atlantic Ocean (CARINA), which has undergone rigorous quality controls [*Olsen et al.*, 2009; *Key*

et al., 2010; *Tanhua et al.*, 2010]. The data can be downloaded from CDIAC (http://cdiac.ornl.gov/oceans/CARINA/Carina_inv.html). We have extracted the most recent data from the Nordic Seas included in CARINA. These are three cruises from 2002 and 2003, covering all gateways to the region (Figure 1): the I/B Oden 2002 (EXPOCODE 77DN20020420), R/V Knorr 2002 (316N20020530), and R/V G.O. Sars 2003 (58GS20030922). For more information about the Nordic Seas CARINA and the analytical methods of the carbon species and related variables the reader is referred to *Olsen et al.* [2009] and references therein. In this work we used dissolved inorganic carbon (DIC), total alkalinity (TA), and hydrography as well as chlorofluorocarbon (CFC) data for estimating water mass ages and calculating C_{ant} (see section 4 and Appendix A). Values of dissolved organic carbon (DOC), burial of particulate organic carbon (POC), and calcium carbonate ($CaCO_3$) were taken from the literature and are further described in sections 4.1.7 and 4.2).

[7] All carbon system calculations were carried out using CO2sys [*Lewis and Wallace*, 1998], and the constants of *Mehrbach et al.* [1973], refit by *Dickson and Millero* [1987]. An exception was for the runoff where the constants of *Millero* [1979] were used.

4. Methods

[8] To evaluate the different sources and sinks of carbon we compile a carbon budget for the Nordic Seas. In this section we will describe all terms of the budget. The resulting gross and net fluxes are presented in section 5.

[9] The carbon budget of the Nordic Seas is defined through the equation:

$$\sum_{i=1}^{n} \rho_i \times V_i(DIC_i + DOC_i) + F_{bur}^{POC} + F_{bur}^{CaCO_3} + F_{air-sea} = \frac{\Delta C_{inv}}{\Delta t} \quad (1)$$

where, the first term ($\Sigma\rho_i \times V_i(DIC_i + DOC_i)$ represents all advective sources (positive) and sinks (negative) of carbon (including rivers and sea ice), the following two terms (F_{bur}^{POC} and F_{bur}^{CaCO3}) represent the loss of carbon through burial in the sediments, the fourth term ($F_{air\text{-}sea}$) is the total air-sea exchange of carbon over the Nordic Seas, and the last term ($\Delta C_{inv}/\Delta t$) represents temporal changes in the total carbon inventory of the Nordic Seas, i.e., storage. In equation (1) ρ_i is the density and V_i is the volume transport of each of the n sources/sinks. We assume that the supply of particulate carbon is negligible compared to the other sources since DOC generally accounts for more than 90% of the organic material in oceanic waters [e.g., *Wheeler et al.*, 1996, 1997; *Kivimäe et al.*, 2010].

[10] To assess the age and associated concentration of C_{ant} in the water masses we adopted the transit-time distribution (TTD) approach [e.g., *Hall et al.*, 2002; *Waugh et al.*, 2006], using CFC-12. The method is described in more detail in Appendix A. For the freshwater sources we used CO2sys [*Lewis and Wallace*, 1998], and the amount of C_{ant} was calculated as the difference in DIC between preindustrial and present (2002) partial pressure of CO_2 (pCO_2), at the given freshwater TA, assuming equilibrium with atmospheric CO_2. The concentrations of preindustrial (PI) DIC that are presented in this paper were simply calculated by subtracting the C_{ant} concentrations from the contemporary DIC concentrations for each source.

[11] We assume the budget to be representative of a mean state of the Nordic Seas in the early 2000s and that there are no correlations between the respective carbon concentrations and associated volume transports. The uncertainties for the individual fluxes include both those following from the distribution of carbon concentrations within each sink/source, and those following from observed variability in volume transport (Tables 1 and 2 and section B2). To assess a reasonable uncertainty in the overall budget, i.e., the uncertainty in our resulting net fluxes, we take volume conservation into account. This is discussed in sections 6 and B3.

[12] We have not put any constraints on the salt budget, and the presented values of mass and salt transports results in a net salt flux of $-3.4\ 10^6$ kg s^{-1} (Table 3). However, the uncertainty in this number is $\pm 2.7\ 10^6$ kg s^{-1} (corresponding to ±80%) when mass balance is included. We will regard this imbalance as an insignificant source of error in the calculations, in comparison to other uncertainties in the presented budget. Each of the terms in the budget will be described in the following sections.

4.1. Advective Terms

[13] These terms include all flows of water into and out of the Nordic Seas, i.e., exchanges with the surrounding ocean areas as well as river runoff and sea ice transport (Table 1). For the exchanges, carbon fluxes are computed by combining volume transports (V) from the literature with carbon concentrations from the CARINA data (DIC) and literature (DOC). The exchange through the Fram Strait will be described at the end (section 4.1.6) since this will partly be tuned to balance the mass budget. Ranges of annual mean transports as published in the literature are used as an estimate of the uncertainty in the respective volume transports; see Table 1 for a summary.

4.1.1. Southern Inflow of Atlantic Water

[14] The southern inflow, which transports AW into the Nordic Seas occurs in three branches: (i) between the Faroes and the Shetland Islands, (ii) across the Iceland-Faroe Ridge (IFR) and (iii) west of Iceland. The volume transports of the branches have been estimated at 3.8, 3.8 and 0.8 Sv (1 Sv = 10^6 m^3 s^{-1}), respectively [*Østerhus et al.,* 2005], and these numbers are adopted in this study. For the Faroe branch the uncertainty has been determined to be on the order of ±0.5 Sv [*Hansen et al.*, 2003] and we adopt the same number for the Shetland branch. The uncertainty in the Iceland branch has been estimated to be on the order of ±20% [*Jónsson and Valdimarsson*, 2005] corresponding to ±0.2 Sv.

[15] We define this inflow as water with $\sigma_\theta \leq 27.8$ kg m^{-3} and $\Theta \geq 3$°C, following *Eldevik et al.* [2009]. In addition, the AW at the IFR has been restricted to salinities ≥35 in order to exclude the Modified East Icelandic Water that occurs in this section. The position of each of these branches as identified in our data, is illustrated in Figures 2–4, which shows the distribution of DIC, C_{ant} and TA across the gateways. The DIC in the inflowing AW is between 2120 and 2140 μmol kg^{-1}. The mean DIC concentration for each branch, including standard deviations, are found in Table 2, as are values for DOC (described more in section 4.1.7), C_{ant}

Table 1. The Water Masses Included in the Nordic Seas Carbon Budget: Definitions and Volume Transports[a]

Area	Water Mass	Water Mass Boundaries	Volume Transport (Sv)	Method	Sources[b]
			Inflows		
DS	AW	$\Theta \geq 3°C$, $\sigma_\theta \leq 27.8$	0.8 ± 0.16[c]	moorings; mean Jan. 1999 – Dec. 2001	1, 2
IFR	AW	$\Theta \geq 3°C$, $S \geq 35$, $\sigma_\theta \leq 27.8$	3.8 ± 0.5	moorings; mean Jan. 1999 – Dec. 2001	1
FSC	AW	$\Theta \geq 3°C$, $\sigma_\theta \leq 27.8$	3.8 ± 0.5	moorings; mean Jan. 1999 – Dec. 2001	1
FS	PW	$\Theta < 0°C$, $\sigma_\theta \leq 27.7$	1.0 ± 0.2	moorings; 1997–2000	3
	MAW	$\Theta > 0°C$, $27.7 < \sigma_\theta \leq 27.97$	1.0 ± 0.2	moorings; 1997–1999	3, 4
	DW	$\Theta < 0°C$, $\sigma_\theta > 27.97$	3.3 ± 1.4	residual calculation in this study	
	Sea ice	$S = 4$	0.1 ± 0.02[d]	sonars; 1990–1997	5
North Sea	NCC	$S = 33.3$	0.65 ± 0.35	geostrophic calculations; annual mean	6
Baltic/Norway	Runoff		0.02 ± 0.003	observational database; 1950–1990	7, 8
All/Greenland	P-E /GIM		0.03[e]		8
Total			14.5 ± 1.7		
			Outflows		
DS	PW	$\Theta < 0°C$, $\sigma_\theta \leq 27.7$	−1.5 ± 0.5	estimated range	9
	OW	$\Theta < 3°C$, $\sigma_\theta > 27.8$	−3.4 ± 0.4	moorings; 1999–2003	10
IFR	OW	$\Theta < 3°C$, $\sigma_\theta > 27.8$	−1.0 ± 0.5	range of observational estimates	11
FSC	OW	$\Theta < 3°C$, $\sigma_\theta > 27.8$	−2.1 ± 0.3	moorings; 1995–2005	11, 12
BSO	AW	$\Theta > 3°C$, $S > 35$	−1.1 ± 0.3	moorings; 1997–2007	13
BSO	NCC	$S < 34.7$	−1.1 ± 0.3	moorings; 1-year mean	14
FS	AW	$\Theta > 0°C$, $27.7 < \sigma_\theta \leq 27.97$	−2.0 ± 0.4	moorings; 1997–2000	3, 4
	DW	$\Theta < 0°C$, $\sigma_\theta > 27.97$	−2.3 ± 0.5	moorings; 1997–1999	3, 4
Total			−14.5 ± 1.1		

[a]Abbreviations: AW, Atlantic Water; BSO, Barents Sea Opening; DS, Denmark Strait; DW, Deep Water; FS, Fram Strait; FSC, Faroe-Shetland Channel; GIM, Greenland ice melt; IFR, Iceland-Faroe Ridge; MAW, Modified Atlantic Water; NCC, Norwegian Coastal Current; P-E, precipitation minus evaporation; PW, Polar Water; OW, Overflow Water.

[b]References: 1, *Østerhus et al.* [2005]; 2, *Jónsson and Valdimarsson* [2005]; 3, *Schauer et al.* [2004]; 4, *Cisewski et al.* [2003]; 5, *Vinje* [2001]; 6, *Gammelsrød and Hackett* [1981]; 7, *Bergström and Carlsson* [1994]; 8, *Dickson et al.* [2007]; 9, *Nilsson et al.* [2008]; 10, *Macrander et al.* [2005]; 11, *Hansen and Østerhus* [2000]; 12, *Hansen and Østerhus* [2007]; 13, *Smedsrud et al.* [2010]; 14, *Skagseth et al.* [2011].

[c]*Jónsson and Valdimarsson* [2005] estimated the uncertainty (1994–2000) to be of the order of 20%.

[d]Standard deviation (~20%) of the mean parameterized flux, tuned with observed values 1990–1997 [*Vinje*, 2001].

[e]No uncertainty was provided by *Dickson et al.* [2007].

Table 2. Mean Values (±1 Standard Deviation) of Carbon in the Different Advective Sources and Sinks Used in the Budget of the Nordic Seas[a]

Area	Water Mass	Density (kg dm^{-3})	DIC (μmol kg^{-1})	DOC[b] (μmol kg^{-1})	TA (μmol kg^{-1})	Mean Age (yr)	C_{ant}[c] (μmol kg^{-1})
			Inflows				
DS	AW	1.0276	2138 ± 3	59 ± 4	2309 ± 2	0 ± 0	48 ± 0
IFR	AW	1.0274	2127 ± 22	58 ± 4	2323 ± 6	4 ± 3	47 ± 3
FSC	AW	1.0273	2121 ± 20	58 ± 4	2325 ± 7	2 ± 2	50 ± 3
FS	PW	1.0270	2133 ± 11	80 ± 10	2270 ± 13	5 ± 4	36 ± 1
	MAW	1.0279	2148 ± 5	62 ± 5	2297 ± 5	28 ± 19	31 ± 5
	DW	1.0281	2154 ± 4	53 ± 3	2300 ± 2	127 ± 91	17 ± 6
	Sea ice		254 ± 4	50 ± 20	270 ± 4	0	4 ± 0
North Sea	NCC[d]	1.026	2037 ± 20	76 ± 8	2241 ± 22	1	43 ± 4
Baltic	Runoff[d]	1	1610 ± 16	355 ± 35	1570 ± 16	0	9 ± 1
Norway	Runoff[d]	1	582 ± 6	334 ± 33	582 ± 6	0	5 ± 0
	P-E/GIM		*negl.*	*negl.*	*negl.*		*negl.*
			Outflows				
DS	PW	1.0274	2114 ± 8	70 ± 10	2266 ± 3	3 ± 1	38 ± 1
	OW	1.0279	2148 ± 6	58 ± 6	2294 ± 5	11 ± 5	37 ± 2
IFR	OW	1.0280	2156 ± 5	53 ± 5	2304 ± 8	21 ± 10	33 ± 4
FSC	OW	1.0280	2163 ± 3	53 ± 5	2303 ± 3	45 ± 22	27 ± 6
BSO	AW	1.0277	2138 ± 15	57 ± 4	2314 ± 6	2 ± 2	46 ± 2
	NCC	1.0268	2083 ± 24	66 ± 7	2287 ± 19	2 ± 2	47 ± 3
FS	AW	1.0279	2142 ± 14	60 ± 5	2306 ± 5	6 ± 5	41 ± 3
	DW	1.0281	2159 ± 5	52 ± 2	2300 ± 3	99 ± 58	19 ± 7

[a]Abbreviations of areas and water masses are found in the caption of Table 1.

[b]For the DOC concentrations of the overflow, river runoff and NCC we have set an uncertainty of 10%.

[c]The value range of the TTD-derived C_{ant} values are here the calculated standard deviation within the defined water masses, in order to show the spread within each source.

[d]For the NCC inflow and the river runoff a DIC/TA uncertainty of 1% has been assumed and the uncertainty in C_{ant} is set to 10%.

Table 3. The Water Masses Included in the Nordic Seas Carbon Budget: Mean Salinity and Salt Transport

Area	Water Mass	Salinity	Salt Transport (10^6 kg s^{-1})
		Inflows	
DS	AW	35.06 ± 0.03	28.8 ± 5.8
IFR	AW	35.18 ± 0.06	137.4 ± 18.1
FSC	AW	35.27 ± 0.11	137.7 ± 18.1
FS	PW	33.58 ± 0.65	34.5 ± 6.9
	MAW	34.83 ± 0.10	35.8 ± 7.2
	DW	34.90 ± 0.01	107.6 ± 51.3
	Sea ice	4	0.4 ± 0.1
North Sea	NCC	33.3	22.2 ± 12.0
Baltic/Norway	Runoff	0	0
All/Greenland	P-E /GIM	0	0
Total			504.4 ± 59.7
		Outflows	
DS	PW	34.07 ± 0.27	−52.5 ± 17.5
	OW	34.86 ± 0.09	−107.5 ± 12.9
IFR	OW	34.89 ± 0.06	−35.9 ± 17.9
FSC	OW	34.91 ± 0.02	−79.0 ± 10.8
BSO	AW	35.09 ± 0.05	−39.7 ± 10.8
BSO	NCC	34.36 ± 0.25	−38.8 ± 10.6
FS	AW	35.01 ± 0.06	−72.0 ± 14.4
	DW	34.92 ± 0.01	−82.6 ± 18.0
	Total		−507.8 ± 40.9

and TA. The AW carries the highest C_{ant} load of all components (~50 μmol kg^{-1}) into the Nordic Seas.

4.1.2. Outflow Across the Greenland-Scotland Ridge

[16] The southern outflows from the Nordic seas are comprised of the surface outflow (PW) in the Denmark Strait, and of dense waters formed north of the ridge. Overflows are defined as water with $\sigma_\theta > 27.8$ kg m^{-3} [e.g., *Saunders*, 1990; *Dickson and Brown*, 1994; *Hansen and Østerhus*, 2000] and $\Theta < 3$°C, where the temperature restriction has been added to exclude occasional influence of inflowing AW [*Eldevik et al.*, 2009]. The transport of dense overflow waters takes place in three branches: (i) 3.4 ± 0.3 Sv across the Denmark Strait [*Macrander et al.*, 2005], (ii) ~1 Sv across the IFR [*Hansen and Østerhus*, 2000], and (iii) 2.2 ± 0.3 Sv with the Faroe-Shetland overflow (consisting of the overflow in the Faroe Bank Channel (1.9 ± 0.3 Sv) [*Hansen and Østerhus*, 2007] and across the Wyville-Thomson Ridge (0.2 ± 0.1 Sv) [*Hansen and Østerhus*, 2000]). The Iceland-Faroe overflow is suggested to be of a somewhat intermittent nature [*Saunders*, 1996; *Hansen and Østerhus*, 2000], and hence large interannual variability is expected. We apply an uncertainty of ±0.5 Sv. The values for volume fluxes and carbon concentrations of the dense overflows are listed in Tables 1 and 2. The dense overflows show increasing values of DIC from the Denmark Strait (2148 μmol kg^{-1}) to the Faroe-Shetland

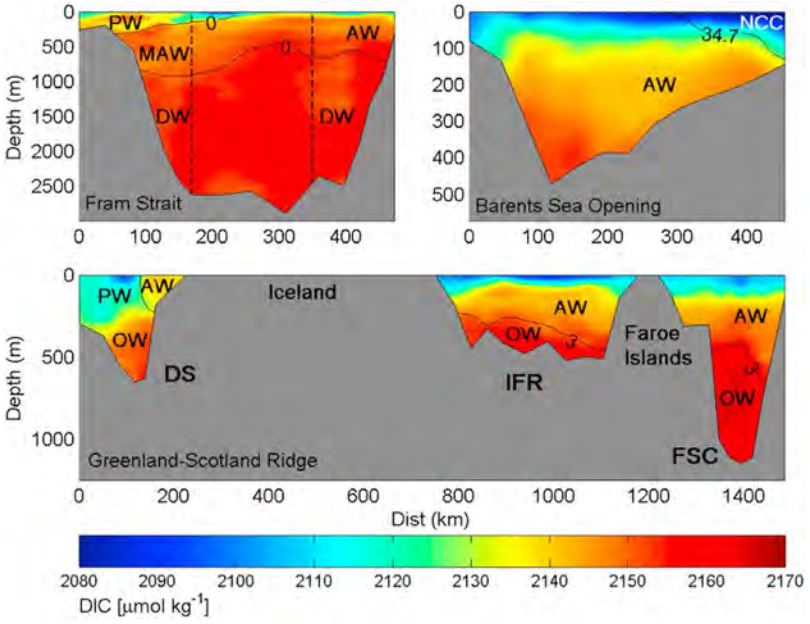

Figure 2. The distribution of dissolved inorganic carbon (DIC) in the gateways: (top left) Fram Strait, (top right) Barents Sea Opening, and (bottom) the Greenland-Scotland Ridge. The dashed lines in FS indicate the borders for the EGC and WSC, respectively (see Figure 1). The solid black lines indicate the borders between the water masses; FS, the 0°C isotherm, separating the Atlantic Waters from the PW and DW; BSO, the 34.7 isohaline that separates the AW from the NCC; GSR, the 3°C isotherm that separates the AW from the PW and the OW. The white dots mark the sample locations. Water mass abbreviations are found in the caption of Table 1 and in section 4.1. Mean values of DIC are found in Table 2. The bottom depths are from the CARINA files. These are either based on recorded bottom depth at each station, or, when this information is lacking, bottom depth was approximated from a global (0.25 degree resolution) topography; see *Key et al.* [2010] for details.

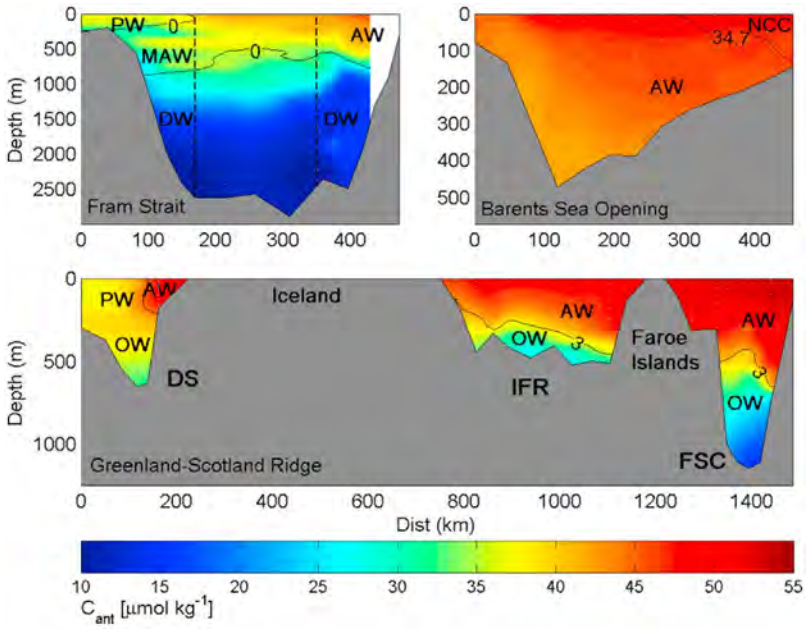

Figure 3. The distribution of anthropogenic carbon (C_{ant}) in the gateways: (top left) Fram Strait, (top right) Barents Sea Opening, and (bottom) the Greenland-Scotland Ridge. The isolines and water masses are the same as in Figure 2. Mean values of C_{ant} are found in Table 2. The white dots mark the sample locations. For information of the bottom depths see caption of Figure 2.

Channel (2163 μmol kg^{-1}), while the concentrations of C_{ant} decrease from west to east (Table 2).

[17] The PW that flows out through the Denmark Strait is defined following *Rudels et al.* [2005] as water with $\Theta < 0$°C, and $\sigma_\theta \leq 27.7$ kg m^{-3}. In contrast to the dense overflows, only a few current measurements in the PW in the Denmark Strait have been reported and estimates vary depending on location and timing of measurements, and on the water mass definition used [*Nilsson et al.*, 2008; *Sutherland and Pickart*, 2008], but a reasonable estimate is in the range of 1–2 Sv (J. Nilsson, personal communication, 2010). We use the mean value of 1.5 Sv, and the range of

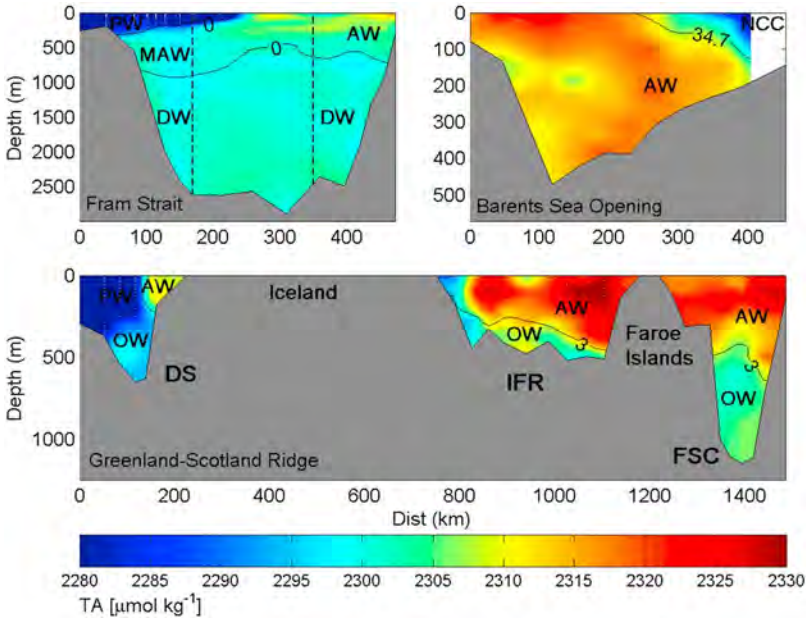

Figure 4. The distribution of total alkalinity (TA) in the gateways: (top left) Fram Strait, (top right) Barents Sea Opening, and (bottom) the Greenland-Scotland Ridge. The isolines and water masses are the same as in Figure 2. Mean values of TA are found in Table 2. The white dots mark the sample locations. For information of the bottom depths see caption of Figure 2.

±0.5 Sv as the uncertainty. The mean DIC concentration in the PW is 2114 μmol kg^{-1}.

4.1.3. Outflow Through the Barents Sea Opening

[18] The eastward flow of AW (S > 35; Θ > 3°C) through the Barents Sea Opening (BSO) has been extensively monitored since 1997 and amounts to 2.0 Sv [*Smedsrud et al.*, 2010]. However, 0.9 Sv of AW recirculates south of Bear Island [*Skagseth*, 2008] resulting in the net outflow of AW through the BSO of 1.1 Sv that is used in the budget. This AW shows a rather large range in DIC concentration, with a mean value of 2138 μmol kg^{-1} (Table 2 and Figure 2). As an uncertainty in the AW outflow through the BSO we adopted the average transport anomaly, from 1997 to 2007 data, of ±0.3 Sv [*Smedsrud et al.*, 2010].

[19] There is also a small inflow of Arctic Water from the Barents Sea, with the Bear Island Current (located in the most northern part of our defined BSO box (see Figure 1) [e.g., *Blindheim*, 1989], but the amount of this transport is presently unknown [*Ingvaldsen et al.*, 2004] and we have neglected this component in the present budget.

4.1.4. Norwegian Coastal Current, Inflow and Outflow

[20] The NCC [*Gammelsrød and Hackett*, 1981; *Björk et al.*, 2001] has been included in the budget. Very few volume transport estimates can be found for the inflowing water (NCC_{IN}) at the southern tip of Norway; we adopt an annual mean value of 0.65 ± 0.35 Sv from *Gammelsrød and Hackett* [1981], and a typical salinity of 33.3 [*Lundberg and Haugan*, 1996]. The NCC exits the Nordic Seas through the BSO (NCC_{OUT}), where it is identified as water with salinity <34.7. The volume transport of that current was recently estimated at 1.1 Sv from a one-year full depth current meter profile in the core of the NCC in the BSO [*Skagseth et al.*, 2011] and we adopt this value in our study. We applied the same uncertainty for the outflow of the NCC as for the outflowing AW in the section (±0.3 Sv).

[21] The DIC concentration in the NCC_{OUT} is 2083 μmol kg^{-1}. The NCC_{IN}, however, is not covered by the CARINA data. To assess the concentration of carbon in this source we used an assumed mixing between the AW and the NCC along the Norwegian coast, based on the salinity difference between the inflowing and the outflowing NCC; 33.3 and 34.36, respectively. To arrive at the salinity of the NCC_{OUT} we need a mixing of 54% AW (with S = 35.27) and 46% NCC_{IN}. This agrees well with the findings of *Gascard et al.* [2004] that about half of the radionuclide Iodine-129 (^{129}I), mainly originating from La Hague, was transferred from the NCC to the AW along the Norwegian coast. These fractions are then used when back-calculating the carbon concentrations in the NCC_{IN} from the AW and the NCC_{OUT}. This gives a DIC concentration in the NCC_{IN} of 2037 μmol kg^{-1}. All resulting carbon concentrations are listed in Table 2.

4.1.5. Freshwater Sources

[22] We also added an import of sea ice through the Fram Strait of 0.1 Sv [*Vinje*, 2001], river runoff of 0.02 Sv (0.01 Sv from Baltic and 0.01 Sv from Norway) [*Bergström and Carlsson*, 1994; *Dickson et al.*, 2007], and an additional 0.03 Sv of non-riverine freshwater (precipitation less evaporation and Greenland ice melt) [*Dickson et al.*, 2007] for the mass budget, but the latter is here neglected as a carbon source.

[23] For the flux of sea ice through Fram Strait, *Vinje* [2001] reported a standard deviation on the order of ±20%, and we use this as the transport uncertainty. For an estimate of the uncertainty in the river runoff we have used *Dickson et al.* [2007] for the Baltic inflow (±15%) and have applied this range also for the runoff from Norway.

[24] For an estimation of the carbon concentrations in the sea ice we follow the approach by *Anderson et al.* [1998], normalizing the DIC values of PW (in Fram Strait) to a mean sea ice salinity of 4 [*Aagaard and Carmack*, 1989]; e.g., $DIC_{sea\ ice} = DIC_{PW} \times (S_{sea\ ice}/S_{PW})$. The other carbon parameters are calculated accordingly (Table 2).

[25] For concentrations of DIC in the Baltic river runoff we use the mean value of the Baltic water flowing into the North Sea (1610 μmol kg^{-1}) from *Hjalmarsson et al.* [2010, Table 1], and for the TA concentration we use the mean surface value of two stations in Baltic Proper (1570 μmol kg^{-1}) [*Hjalmarsson et al.*, 2008, Table 2]. The runoff TA value from Norway is from the salinity/TA relationship in the Atlantic domain assessed by *Nondal et al.* [2009], where the intercept of the fitted line at S = 0 gives a TA value of 582 μmol kg^{-1}. We use the same value for the concentration of DIC following *Anderson et al.* [1998].

4.1.6. Exchange Through the Fram Strait

[26] The exchange through the Fram Strait has been divided into five water masses, following *Schauer et al.* [2004]; an eastern outflow of northward flowing AW and Deep Water (DW) with the WSC, and a western inflow of PW, Modified Atlantic Water (MAW), and DW with the southward flowing EGC. The water masses are indicated in Figures 2–4, and their carbon concentrations are provided in Table 2. To assess the uncertainty in the volume transport estimates for the individual water masses we have largely followed the reported ranges in the observed annual transports between 1997 and 2000 from *Schauer et al.* [2004], which are on the order of ±15–20%. We will here start by describing the outflows.

[27] The northward flow of AW (defined as water with Θ > 0°C and 27.7 < $\sigma_\theta \leq$ 27.97 kg m^{-3}) has been measured to 4 Sv [*Cisewski et al.*, 2003; *Schauer et al.*, 2004]. However, both geostrophic calculations and high-resolution model results have suggested that only 50% of the AW reaching the Fram Strait actually enters the Arctic Ocean [*Rudels,* 1987; *Aksenov et al.*, 2010], while the remainder recirculates in the Fram Strait region. We therefore adopt a net number for AW export through the Fram Strait of 2 ± 0.4 Sv. In addition to the AW, the WSC also carries 4.6 Sv of DW northward [*Schauer et al.*, 2004], where DW is defined as water colder than 0°C and with σ_θ > 27.9 kg m^{-3} [*Rudels et al.*, 2000; *Schauer et al.*, 2004]. Due to the strong barotropic nature of the WSC [*Fahrbach et al.*, 2001; *Schauer et al.,* 2004] we assume that, similar to the AW, half of the northward flowing DW recirculates in the strait and thus we assess a net DW outflow of 2.3 ± 0.5 Sv.

[28] Of the inflows, PW in the EGC has been defined the same way as in the Denmark Strait (Θ < 0°C; $\sigma_\theta \leq$ 27.7 kg m^{-3}) [*Rudels et al.*, 2005] and we have adopted the volume transport estimate of 1 ± 0.2 Sv of *Schauer et al.* [2004]. MAW was defined in the same way as the AW (Θ > 0°C; 27.7 < $\sigma_\theta \leq$ 27.7 kg m^{-3} [e.g., *Rudels et al.*, 2000]) and its volume flux has been estimated to be about 3 Sv [*Cisewski et al.*, 2003; *Schauer et al.*, 2004]. However, the recirculation of 2 Sv of AW mentioned above must be taken into account, leaving 1 Sv of MAW entering the

Nordic Seas from the Arctic Ocean. The reported range in MAW transport is approximately ±20% [*Schauer et al.*, 2004], corresponding to ±0.2 Sv. Finally, the volume transport of the southward flowing DW has to be included, and we will assess this from the assumption of a balanced mass budget. Adding up all volume transports considered until now gives a total inflow of 11.2 ± 0.9 Sv and an outflow of 14.5 ± 1.2 Sv. Thus we need 3.3 ± 1.4 Sv to balance the mass budget, where the uncertainty is the propagated error of the inflows and outflows, assuming they are independent. We adopt this transport for the DW inflow through the Fram Strait. This value corresponds to almost half of the annual average of the observed total southward transport in Fram Strait of ~7 Sv [*Schauer et al.*, 2004].

4.1.7. DOC in the Advective Terms

[29] In addition to the amount of DIC in each component we also need to know the concentration of DOC. We adopt values from the literature, especially *Amon et al.* [2003] and *Benner et al.* [2005], who present values of DOC for different water masses in the Nordic Seas (Table 2). Most of the AW-derived water masses have concentrations close to 60 μmol kg^{-1}, while the denser waters show values just above 50 μmol kg^{-1}. The inflowing PW has the highest concentration (80 μmol kg^{-1}), which has decreased to 70 μmol kg^{-1} when the water leaves the Nordic Seas through the Denmark Strait. For the DOC concentration in the inflowing NCC the value of the Baltic Sea inflow to the North Sea (76 μmol kg^{-1}) presented by *Thomas et al.* [2005] has been used. The DOC concentration in the NCC in the BSO is calculated from a mixing between the inflowing NCC and the eastern branch of inflowing AW (see section 4.1.4). The highest content of DOC is found in the river runoff. The value for the Baltic runoff (355 μmol kg^{-1}) is estimated from *Schneider et al.* [2003] as the average mean surface DOC between March and September 2001, and for the DOC in the runoff from Norway (334 μmol kg^{-1}) we used the salinity-DOC regression from *Børsheim et al.* [1999].

4.2. Burial Terms

[30] Some of the organic carbon sinks to the bottom and get buried in the sediments. The burial rate of organic carbon in the Nordic Seas is estimated to be 0.06 ± 0.01 g C m^{-2} yr^{-1}, which is a mean of the burial rates in the Eurasian Basin of the Arctic Ocean (0.07 g C m^{-2} yr^{-1}) and the Atlantic (0.05 g C m^{-2} yr^{-1}) [*Berner*, 1982]. With a Nordic Seas' area of ~2.8 10^{12} m^2 [*Jakobsson*, 2002] this gives a total burial of about 0.2 Mt C yr^{-1} (1 Mt = 10^6 t). This is ~5% of the total organic carbon reaching the seafloor, seen from the estimated rain rate of carbon between 60 and 80°N, of ~1.3 g C m^{-2} yr^{-1} [*Schlüter et al.*, 2000]. This low degree of burial is consistent with the estimate of the total organic carbon burial rate in the deep global ocean of ~3% of the seafloor deposition rate [*Jahnke*, 1996]. We have neglected any burial of particulate inorganic carbon (PIC) in the budget since a study from the Fram Strait showed that PIC fluxes are only in the order of 10–20% of the POC fluxes [*Bauerfeind et al.*, 2009]. Considering the low amount of POC that is removed from the water column to the sediments, the burial of PIC is within the uncertainty range of our budget.

[31] The mean flux of carbonate in the Arctic/Subarctic area is 1.1 ± 0.9 g C m^{-2} yr^{-1} [*Milliman*, 1993], which results in a total carbonate flux in the Nordic Seas of 3.0 ± 2.6 Mt C yr^{-1}. With an assumed preservation of 80% in the Nordic Seas/Arctic Ocean [*Milliman*, 1993] the annual accumulation of carbonate in the Nordic Seas sediments amounts to 2.4 ± 2.1 Mt C.

[32] The burial rate of organic carbon and carbonate add up to a total carbon burial of 2.6 ± 2.1 Mt C yr^{-1} in the Nordic Seas.

4.3. Storage

[33] For the budget we also need to assess the accumulation, or storage, of carbon as a result of the increasing atmospheric pCO_2 due to anthropogenic emissions. To achieve this we adopt the concept of transient steady state [e.g., *Gammon et al.*, 1982]. This states that for tracers with exponentially increasing surface water concentrations the vertical tracer profiles will reach a "transient steady state." Then the tracer concentrations at all depths will change proportionally to the change in surface concentrations. This allows for scaling of C_{ant} concentrations between different years. The Nordic Seas' inventory of C_{ant} in 2002 was recently estimated by *Olsen et al.* [2010] to 1.24 Gt (with lower and upper bounds of 0.9 and 1.4 Gt C_{ant}, respectively). The pCO_2 in the atmosphere in 2002 was 373.1 ppm, and the atmospheric pCO_2 in 1980 (which is here chosen as a reference year) was 338.7 ppm. These values are compared to the preindustrial (PI) value of 280 ppm. For waters in equilibration with the atmosphere, we find that the PI, 1980, and 2002 pCO_2 values correspond to DIC concentrations of 2131.3, 2160.1, and 2174.4 μmol kg^{-1}, respectively. For these calculations we used median values for salinity, temperature, TA, silicate and phosphate, calculated from all CARINA data within the Nordic Seas (1982–2003), of, 34.898, −0.170°C, 2296.9 μmol kg^{-1}, 5.930 μmol kg^{-1}, and 0.850 μmol kg^{-1}, respectively. The excess concentrations of DIC in 1980 and 2002 were simply taken as the difference between the respective DIC concentration, and the PI level (hence, DIC excess in 1980 = DIC_{1980}-DIC_{PI}, and the same for the 2002 value). This gives that the excess in 1980 was 67.5% of the 2002 level. From this we multiply the 2002 inventory from *Olsen et al.* [2010] with 0.675 to get the inventory in 1980, assuming transient steady state. From this the annual change in storage between 1980 and 2002 is 0.018 Gt C yr^{-1} (with lower and upper bounds of 0.013 and 0.021 Gt C yr^{-1}, respectively). This storage agrees with the storage rate *Pérez et al.* [2010] calculated from the Nordic Seas inventory of 1.2 Gt C estimated by *Jutterström et al.* [2008], using a correction proposed by *Tanhua et al.* [2007]. One error source to the scaling approach is temporal changes in seawater buffer capacity, but this has been shown to have negligible effect on the calculations [*Tanhua et al.*, 2007].

4.4. Air-Sea Flux

[34] The remaining part in the budget to estimate is then the air-sea flux of CO_2, which will be determined as the residual of the other fluxes. This value will be compared with that extracted from the pCO_2 and air-sea CO_2 flux climatology from *Takahashi et al.* [2009], obtained from

Table 4. Advective Transports of Dissolved Carbon in the Nordic Seas[a]

Area	Water Mass	DIC Flux (Gt C yr^{-1})	TA Flux (Gt C yr^{-1})	C_{ant} Flux[b] (Gt C yr^{-1})	DOC Flux (Gt C yr^{-1})	Total C Flux (Gt C yr^{-1})
			Inflows			
DS	AW	0.67 ± 0.13	0.72 ± 0.14	0.015 ± 0.004	0.019 ± 0.004	0.69 ± 0.13
IFR	AW	3.15 ± 0.42	3.44 ± 0.45	0.070 ± 0.013	0.087 ± 0.013	3.24 ± 0.42
FSC	AW	3.14 ± 0.41	3.44 ± 0.45	0.075 ± 0.013	0.087 ± 0.013	3.23 ± 0.41
FS	PW	0.83 ± 0.17	0.88 ± 0.18	0.015 ± 0.004	0.032 ± 0.007	0.86 ± 0.17
	MAW	0.84 ± 0.17	0.90 ± 0.18	0.013 ± 0.003	0.024 ± 0.005	0.86 ± 0.17
	DW	2.77 ± 1.20	2.96 ± 1.28	0.025 ± 0.012	0.069 ± 0.030	2.84 ± 1.20
	Sea ice	0.01 ± 0.002	0.01 ± 0.002	$0.0002 \pm 3.7\ 10^{-5}$	0.002 ± 0.001	0.012 ± 0.002
North Sea	NCC	0.52 ± 0.28	0.57 ± 0.31	0.011 ± 0.006	0.020 ± 0.011	0.54 ± 0.28
Baltic	Runoff	0.006 ± 0.001	0.006 ± 0.001	$3.6\ 10^{-5} \pm 6.3\ 10^{-6}$	$1.4\ 10^{-3} \pm 2.4\ 10^{-4}$	0.007 ± 0.001
Norway	Runoff	0.002 ± 0.0003	0.002 ± 0.0003	$1.8\ 10^{-5} \pm 3.1\ 10^{-6}$	$1.3\ 10^{-3} \pm 2.3\ 10^{-4}$	0.003 ± 0.0004
Total in		11.94 ± 1.39	12.93 ± 1.49	0.225 ± 0.024	0.343 ± 0.037	12.28 ± 1.39
			Outflows			
DS	PW	−1.24 ± 0.41	−1.32 ± 0.44	−0.023 ± 0.008	−0.043 ± 0.015	−1.28 ± 0.41
	OW	−2.85 ± 0.30	−3.04 ± 0.32	−0.050 ± 0.010	−0.078 ± 0.011	−2.92 ± 0.30
IFR	OW	−0.84 ± 0.42	−0.90 ± 0.45	−0.014 ± 0.007	−0.022 ± 0.011	−0.86 ± 0.42
FSC	OW	−1.77 ± 0.25	−1.89 ± 0.27	−0.022 ± 0.006	−0.044 ± 0.008	−1.81 ± 0.25
BSO	AW	−0.92 ± 0.25	−0.99 ± 0.27	−0.020 ± 0.006	−0.025 ± 0.007	−0.94 ± 0.25
	NCC	−0.89 ± 0.24	−0.98 ± 0.27	−0.021 ± 0.006	−0.029 ± 0.008	−0.92 ± 0.24
FS	AW	−1.67 ± 0.33	−1.80 ± 0.36	−0.032 ± 0.008	−0.047 ± 0.010	−1.72 ± 0.33
	DW	−1.93 ± 0.42	−2.06 ± 0.45	−0.017 ± 0.007	−0.046 ± 0.010	−1.98 ± 0.42
Total out		−12.11 ± 0.95	−12.98 ± 1.02	−0.202 ± 0.021	−0.335 ± 0.029	−12.45 ± 0.95

[a]The presented uncertainties in the transport values are the propagated errors, calculated both from the standard deviations of the respective parameter, within the respective water masses, and individual uncertainties in the volume transports (see Appendix B). Abbreviations of areas and water masses are found in the caption of Table 1. See text for details.

[b]The uncertainties in the TTD-based C_{ant} fluxes were determined from propagation of uncertainties in the TTD method [*Waugh et al.*, 2006] and standard error of the mean concentrations, while the errors in the values for NCC inflow, ice and river runoff are set to 10% (see section B1).

http://www.ldeo.columbia.edu/res/pi/CO2/carbondioxide/pages/air_sea_flux_2000.html.

5. Results

5.1. Carbon Transports

[35] The advective carbon transports in this work are summarized in Table 4. Presently, 12.3 ± 1.4 Gt of total carbon (i.e., DIC + DOC) are transported into the Nordic Seas each year, while 12.5 ± 0.9 Gt C exit the region. The uncertainties presented include the estimated uncertainties in the individual volume transports. Despite this the total transport uncertainty in and out of the region is not larger than ~10%. The transport of DIC dominates the horizontal fluxes of carbon (>97%), which is consistent with the estimates of the flow through the Barents Sea [*Kivimäe et al.*, 2010]. There is net DIC inflow across the Iceland-Scotland Ridge (3.7 Gt C yr^{-1}) and through the Fram Strait (0.8 Gt C yr^{-1}), while there are net outflows through the Denmark Strait (−3.4 Gt C yr^{-1}) and through BSO (−1.8 Gt C yr^{-1}) (Figure 5). The two largest branches of AW, east of Iceland, are responsible for 50% of the inflowing carbon, while 45% of the total carbon that leaves the area follows the dense overflows into the deep parts of the North Atlantic. For NCC, the DIC is increasing during the northward transport along the Norwegian coast (from 2037 μmol kg^{-1} in the south to 2083 μmol kg^{-1} in BSO), due to the solubility pump and the relatively strong mixing with AW [*Mauritzen*, 1996; *Gascard et al.*, 2004; *Nilsen and Falck*, 2006].

[36] The transport of C_{ant} is even more strongly related to the main inflowing branches of AW than the transport of DIC; these waters carry more than 60% of the total inflow of ~0.22 Gt C_{ant} yr^{-1}, but almost 40% of this amount exits the Nordic Seas with AW through BSO and the Fram Strait (Figure 5 and Table 4). The C_{ant} transported out of the Nordic Seas with the dense overflows is most strongly connected (~60%) to the Denmark Strait overflow, consistent with the markedly younger mean age of the western overflow compared to the eastern (Table 2). The higher age and lower concentrations of C_{ant} found in the eastern overflows are attributed to the relatively large admixture of older deep water from the Norwegian Sea [*Turrell et al.*, 1999] (Figure 3). The greater depth of the Faroe Channels compared with the relatively shallow Denmark Strait also allows a larger fraction of denser water in the former overflow. This conclusion is also supported by a water mass analysis of 2002 data at the Denmark Strait sill [*Jeansson et al.*, 2008], where the contribution of deep water to the Denmark Strait overflow ($\sigma_\theta > 27.8$ kg m^{-3}) was insignificant.

[37] In the Fram Strait MAW shows a clearly lower concentration of C_{ant} compared to the northward flowing AW, following the significantly greater age of MAW, which is attained after one or several loops in the Arctic Ocean [e.g., *Rudels et al.*, 1999].

[38] The concentrations of TA are strongly correlated with the salinity [see, e.g., *Bellerby et al.*, 2005; *Nondal et al.*, 2009] (see also Tables 2 and 3), and hence the inflow of AW across the eastern part of the GSR has the highest alkalinity of all water masses (Figure 4), while it is lower in AW that exits the region through the BSO and the Fram Strait, as a result of the mixing with NCC waters along the Norwegian coast, and with ambient less saline water in the Nordic Seas [e.g., *Mauritzen*, 1996]. The dense overflows carry TA levels that fall in between those of AW and PW, with the Denmark Strait overflow having lower concentrations than the overflows east of Iceland, in agreement with

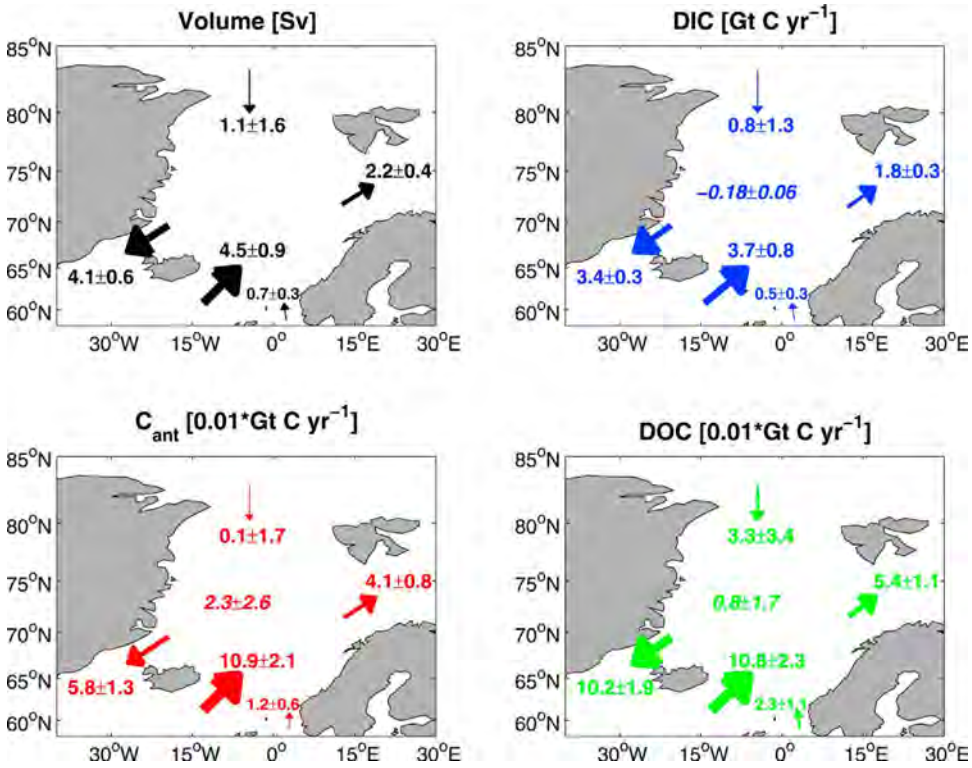

Figure 5. Net transports of volume and carbon in the gateways connecting the Nordic Seas with the surrounding ocean areas. The maps show the transports of (top left) volume, (top right) DIC, (bottom left) C_{ant}, and (bottom right) DOC. Units are Sv for the volume transports and Gt C yr^{-1} for the carbon transports. The total net transport of the respective carbon specie is shown in italic numbers; positive values indicate net transport into the Nordic Seas and negative values out of the region. Note that the transport values for C_{ant} and DOC are given in hundredths of Gt C yr^{-1}.

the decreasing east-west salinity gradient. The net TA transports through the openings are very similar to the net transports of DIC, and will not be shown here.

5.2. Carbon Budget for the Nordic Seas

[39] Summarizing all advective transports of dissolved carbon, including the river runoff and total burial rate, results in a total net flux out of the Nordic Seas of 0.17 ± 0.06 Gt C yr^{-1}. (The uncertainty follows from the assumption of volume balance; see section B3. It should be noted that the propagated error, when treating all volume transports as uncorrelated, results in a total error as large as ±1.7 Gt C yr^{-1}. We argue that this is unrealistically large for the net flux of carbon in the Nordic Seas as discussed in sections 6 and B3.) The net advective transport of DIC is balanced by the storage of C_{ant} and the air-sea flux of CO_2. Combining the net transport of carbon and the storage (equation (1)) results in an uptake of atmospheric CO_2, in 2002, in the Nordic Seas of 0.19 ± 0.06 Gt C yr^{-1}, or 0.2 ± 0.1 Gt C yr^{-1}.

[40] There is a small net advective transport of C_{ant} into the Nordic Seas of 0.023 ± 0.026 Gt C yr^{-1}. Considering the magnitude of the uncertainty this may not be significant, however, it agrees with our estimated storage of C_{ant} in the Nordic Seas (0.021 Gt C yr^{-1}), suggesting that there is negligible uptake of C_{ant} from the atmosphere in the Nordic Seas, i.e., advection of C_{ant} with the inflowing AW across the GSR is responsible for the net accumulation of C_{ant} in the Nordic Seas and the Arctic Ocean. The overturning circulation in the Nordic Seas redistributes much of the C_{ant} entering the region with the AW, and part of this then exits the Nordic Seas with the dense overflows [*Olsen et al.*, 2010]. It is beyond the scope of this paper to quantify the amount of C_{ant} taking part in this loop, and the sources to the overflows. However, the total amount of C_{ant} transported within the dense overflows (almost 0.09 Gt C yr^{-1}) is about 50% of the C_{ant} inflow with AW across the GSR (~0.16 Gt C yr^{-1}) (cf. Table 4).

[41] For an estimation of the preindustrial (or natural) carbon budget (Table 5) we assume a system in steady state and hence the fluxes of TA, organic carbon, and the burial rate are assumed to be the same as today. Since the storage equals zero in preindustrial times the sum of the preindustrial advective transports, including the river runoff and burial rate, gives an air-sea exchange for the preindustrial carbon system in the Nordic Seas of −0.20 ± 0.08 Gt C yr^{-1}. Neither the net flux of TA (−0.05 ± 0.34 Gt C yr^{-1}) nor the net flux of DOC (0.01 ± 0.02 Gt C yr^{-1}) is significantly different from zero. We will not discuss these fluxes further in this paper.

6. Discussion

[42] The carbon budget illustrates the importance of the exchange of carbon between the Nordic Seas and the North Atlantic across the GSR, and with the Arctic Ocean through the BSO and the Fram Strait. The net inflow across the

Table 5. The Pre-Industrial (PI) Advective Transports of Dissolved Inorganic Carbon for the Nordic Seas[a]

Area	Water Mass	DIC (μmol kg^{-1})	C_{ant} (μmol kg^{-1})	PI DIC[b] (μmol kg^{-1})	PI DIC Flux[c] (Gt C yr^{-1})
			Inflows		
DS	AW	2138 ± 3	48 ± 0	2090 ± 3	0.65 ± 0.13
IFR	AW	2127 ± 22	47 ± 3	2080 ± 25	3.08 ± 0.42
FSC	AW	2121 ± 20	50 ± 3	2071 ± 23	3.07 ± 0.41
FS	PW	2133 ± 11	36 ± 1	2097 ± 12	0.82 ± 0.17
	MAW	2148 ± 5	31 ± 5	2117 ± 10	0.83 ± 0.17
	DW	2154 ± 4	17 ± 6	2137 ± 10	2.75 ± 1.20
	Sea ice	254 ± 4	4 ± 0	249 ± 4	0.01 ± 0.002
North Sea	NCC	2037 ± 20	43 ± 4	1994 ± 25	0.51 ± 0.28
Baltic	Runoff	1610 ± 16	9 ± 1	1601 ± 18	0.006 ± 0.001
Norway	Runoff	582 ± 6	5 ± 0	577 ± 7	0.002 ± 0.0003
Total in					11.73 ± 1.39
			Outflows		
DS	PW	2114 ± 8	38 ± 1	2076 ± 9	−1.22 ± 0.41
	OW	2148 ± 6	37 ± 2	2111 ± 8	−2.80 ± 0.30
IFR	OW	2156 ± 5	33 ± 4	2123 ± 9	−0.83 ± 0.42
FSC	OW	2163 ± 3	27 ± 6	2136 ± 9	−1.75 ± 0.25
BSO	AW	2138 ± 15	46 ± 2	2092 ± 17	−0.90 ± 0.25
	NCC	2083 ± 24	47 ± 3	2036 ± 27	−0.88 ± 0.24
FS	AW	2142 ± 14	41 ± 3	2101 ± 17	−1.64 ± 0.33
	DW	2159 ± 5	19 ± 7	2139 ± 12	−1.92 ± 0.42
Total out					−11.93 ± 0.95

[a]Abbreviations of areas and water masses are found in the caption of Table 1.

[b]The PI DIC concentrations are simply the measured DIC concentrations with the concentration of C_{ant} subtracted.

[c]The uncertainties in the flux values are given from the propagated errors of the DIC and the C_{ant} fluxes (see Table 4).

GSR, together with the NCC, annually adds 0.8 Gt DIC and ~0.06 Gt C_{ant} (Figure 5) to the Nordic Seas and the Arctic Ocean. The budget suggests that 1.0 Gt DIC and 0.04 Gt C_{ant} are annually exported to the Arctic Ocean, via the Barents Sea (Figure 5). The northward transport of C_{ant} corresponds to 64% of the net southern inflow of C_{ant}, hence leaving 36% in the Nordic Seas, as storage. The variability of the storage and the associated transports should be evaluated further in future studies as it is anticipated that the region will become a net source of C_{ant} [*Bellerby et al.*, 2005].

[43] The southern outflow of C_{ant} across the GSR, mostly associated with the dense overflows, contributes to the sequestering of C_{ant} in the North Atlantic. We assess that 0.09 Gt C_{ant} is annually exported from the Nordic Seas into the deep North Atlantic with the dense overflows, corresponding to almost 4% of the annual global ocean uptake of C_{ant} [*Gruber et al.,* 2009]. Our estimate is in good agreement with the estimate of *Olsen et al.* [2010] of 0.06–0.07 Gt C. *Pérez et al.* [2010] estimated a storage rate in the North Atlantic of 0.054 ± 0.006 Gt C yr^{-1} (when high NAO phase was dominant, 1991–1997) but only 0.026 ± 0.004 Gt C yr^{-1} when low NAO phase dominated, 1997–2006. From a water mass analysis of 2002 data in the East Greenland Current, *Jutterström and Jeansson* [2008] estimated that approximately 0.04 Gt C yr^{-1} is transported with the DSOW across the GSR (consistent with the estimate we present here, of 0.05 ± 0.01 Gt C yr^{-1}), and *Jeansson* [2005] estimated a similar transport with the ISOW (including both eastern overflows; IFR and FSC). This range of studies show the general agreement in the estimates of C_{ant} with the dense overflows from the Nordic Seas, and their contribution to the North Atlantic carbon storage, but also indicate that more studies are needed to understand the variability of the transport in and out of the Nordic Seas related to different forcing mechanisms, for example the North Atlantic Oscillation, affecting both the Atlantic inflow [*Blindheim et al.*, 2000] and the circulation of denser waters within the Nordic Seas [*Eldevik et al.*, 2005].

[44] It is important to quantify and understand the uncertainty in the net carbon transports due to the variability in the different sinks and sources. The uncertainties for all individual carbon transports are shown in Table 4. The total uncertainty deduced solely from the uncertainty in the individual carbon concentrations (cf. Table 2) is ±0.06 Gt C yr^{-1}, corresponding to 40% of the estimated net transport. However, the largest uncertainties in the budget are related to the variability in the volume transports. For example, the observed interannual variability in Atlantic inflow and dense overflows across the GSR are about 10% [*Quadfasel and Käse*, 2007; *Hansen et al.*, 2008]. This transport variability implies anomalous carbon transports of some 0.5 Gt C yr^{-1} with the inflow and overflows of individual branches, much larger than the ~1% uncertainty associated with the observed total carbon concentrations. We here also want to evaluate the uncertainty in the net carbon transport, and related CO_2 uptake, associated with the observed variability in ocean volume transports. This has to take conservation of mass into account; otherwise the resulting error estimate will be unrealistically large. A mass-conserving framework for assessing the uncertainty in net carbon transport is presented in section B3. The constrained uncertainty is 0.06 Gt C yr^{-1}, an order of magnitude less than that associated with individual branches, and in line with that associated with uncertain carbon concentrations alone. Thus our best estimate of the present CO_2 uptake in the Nordic Seas is 0.2 ± 0.1 Gt C yr^{-1}. This estimate is consistent with the estimates from *Skjelvan et al.* [2005], of 0.09 ± 0.01 Gt C yr^{-1}, and *Takahashi et al.* [2009], of 0.11 ± 0.06 Gt C yr^{-1}, taken into account the estimated uncertainty.

[45] One caveat for the presented budget is related to the fact that most of the available carbon and carbon-related data for the Nordic Seas are collected during the summer season. Due to this we likely have underestimated the carbon transports in the surface waters since their carbon concentrations will be higher in winter. Since the surface waters dominate the inflow this would give a larger transport of carbon to the Nordic Seas. This would decrease the net outflow of the region, and hence also the balancing CO_2 uptake. More winter data would increase the understanding of seasonal variability of the carbon system, and the associated carbon transport in the region.

[46] The largest uncertainty in the presented carbon budget is connected to the uncertainty in the mass transport in Fram Strait, as illustrated in the net transports in Figure 5. The small uncertainty in the individual mean DIC concentrations (<0.7%) in the exchanging water masses in the strait (assessed from the respective standard deviations of the DIC values; Table 2), however, indicates that the water masses are relatively homogenous with respect to DIC. The largest spread in the inflowing DIC values (~1%) are found in the main AW branches at the GSR, and similar uncertainties are seen in the AW flowing out of the region through

the BSO and the Fram Strait, and also the outflowing NCC in the BSO. The largest uncertainties in the C_{ant} concentrations are found in water masses with a large range in mean age (DW in the Fram Strait and overflow through the FSC; see discussion in section B1), reaching the order of ±20%. Dividing the Fram Strait deep water into both intermediate and deep components would give more representative concentrations of C_{ant} in each of these waters. However, the volume transports are presently not known well enough to make such a distinction. We have thus tried to follow the definitions made for the different volume transport estimates to avoid additional uncertainties. The uncertainty connected to the spread of carbon concentrations within all individual water masses has already been discussed above, from the error propagation, and the fact that the total error from this uncertainty is not larger than ±0.06 Gt C yr^{-1}, gives us faith that the presented water mass concentrations are reasonable.

[47] The present (2002) air-sea flux determined in this study is not significantly different from the calculated mean preindustrial value, which agrees with the findings of *Lundberg and Haugan* [1996]. The net advective transport from the Nordic Seas, however, is smaller during industrial periods due to the accumulation of C_{ant}.

[48] Interannual variability of the air-sea flux of CO_2 in the northern North Atlantic of up to ±20% has been calculated for the period between 1981 and 2001 [*Olsen et al.*, 2003] and the North Atlantic shows larger interannual variability in the uptake than anticipated [*Watson et al.*, 2009]. It is yet too soon to conclude whether the observed decrease in the North Atlantic CO_2 uptake [*Schuster et al.*, 2009] is a persistent trend, but this and the study by *Watson et al.* [2009] strengthens the importance of a more comprehensive observation system in the North Atlantic area since this is one of the main uptake regions of CO_2 in the global ocean.

[49] Recently *Arrigo et al.* [2010], using remote sensed data of sea ice and chlorophyll *a*, and modeled fields of temperature and salinity, estimated the net sink of CO_2 in the Arctic Mediterranean, north of the Arctic Circle (~66°N), during 1998–2003 to 118 ± 7 Tg C yr^{-1} (1 Tg = 10^{12} g), or ~0.12 Gt C yr^{-1}, which is in very good agreement with the estimate provided by *Lundberg and Haugan* [1996] of 0.11 Gt C yr^{-1} for the Nordic Seas and the Arctic Ocean. However, the estimated CO_2 uptake in Arrigo et al.'s 'Greenland sector', covering most parts of the Nordic Seas and extending into the Arctic Ocean, was on average ~0.04 Gt C yr^{-1}, which is clearly lower than any of the estimates for the Nordic Seas (see discussion earlier). An important question is also how the CO_2 fluxes in these regions will be affected in a changing climate. *Jutterström and Anderson* [2010] estimated that the projected decrease in summer sea ice cover in the Arctic Ocean can result in a potential increase in CO_2 uptake of 1.3 ± 0.3 Tg C yr^{-1}, much due to the present undersaturation of Arctic Ocean surface waters with respect to pCO_2. From this the authors estimated a total uptake capacity, over the deep central Arctic Ocean, of 63 ± 14 Tg C. The Arctic Ocean is also affected by the large inflow of freshwater from the Russian rivers and the associated transport of DOC and this is likely to increase in a warmer climate. How this will affect the Arctic Ocean carbon cycle needs to be monitored and evaluated thoroughly. The Nordic Seas CO_2 sink, on the other hand, will likely be less affected than the Arctic Ocean, which largely is due to the fact that most parts of the Nordic Seas are ice free. The most direct effect will be linked to changes in the inflowing Atlantic Water, and then especially the amount of anthropogenic CO_2, and the resulting storage. This highlights the need for continued monitoring of the Nordic Seas gateways, both of the volume fluxes and of the oceanic carbon system. This could unravel the interannual and seasonal signals and would decrease the overall uncertainties in the carbon fluxes. The present study is an improvement in this direction, serving as a benchmark for future observational and modeling studies of the Nordic Seas carbon fluxes.

7. Concluding Remarks

[50] The horizontal advection of carbon is clearly dominating the carbon fluxes in the Nordic Seas with an inflow of 12.3 ± 1.4 Gt yr^{-1} of total carbon (i.e., DIC + DOC) and an outflow of 12.5 ± 0.9 Gt C yr^{-1}. Presently the Nordic Seas annually take up 0.2 ± 0.1 Gt CO_2 from the atmosphere. The budget suggests that there is little or no air-sea exchange of C_{ant} in the Nordic Seas, but approximately 0.02 Gt C_{ant} is accumulated in the subsurface waters annually. There is no significant difference between the 2002 and preindustrial uptake of CO_2 in the Nordic Seas, but the net advective transport of carbon out of the region is smaller today due to the accumulation of anthropogenic CO_2.

[51] The uncertainties in the presented advective carbon transports exchanged through the Nordic Seas gateways include observed uncertainties in both carbon concentrations and volume transports, and are presently about 10% of the gross fluxes. The uncertainty in the net transport of carbon, when mass conservation is applied, is ±0.06 Gt C yr^{-1}, which corresponds to approximately ±30% of the net flux.

Appendix A: Assessment of C_{ant} From Transient Time Distributions

[52] The transit-time distribution (TTD) method [e.g., *Hall et al.*, 2002; *Waugh et al.*, 2006] is based on measurements of transient tracers and a transfer function (the TTD) to scale the tracer concentrations to C_{ant}. It is assumed that the TTDs can be approximated by inverse Gaussian functions, where the mixing can be represented by the mean transit time ("mean age"; Γ) and the width of the TTD (Δ) [e.g., *Waugh et al.*, 2004]. The Δ/Γ ratio indicates the importance of mixing, where $\Delta/\Gamma = 0$ is a purely advective flow. In this study we use a mixing ratio of 1, which have been found to best describe the data in the Nordic Seas [*Olsen et al.,* 2010], and also in the North Atlantic [*Waugh et al.,* 2004] and the Arctic Ocean [*Tanhua et al.,* 2009]. This assumption implies rather strong mixing, resulting in wide age spectra, and hence the uncertainty in the age estimate is relatively large. We have adopted a time-dependent surface saturation of CFC-12 demonstrated by *Tanhua et al.* [2008] for the North Atlantic, and also applied to the Arctic Ocean [*Tanhua et al.,* 2009], which assumes that the saturation was 86% up to 1989 and then increased linearly to 1999 when it reached 100%. For the calculation of preformed TA, i.e., the surface TA at the time

of formation, we use the salinity-TA relationships suggested by *Nondal et al.* [2009].

Appendix B: Uncertainties in the Carbon Fluxes

[53] In the following sections we will estimate the uncertainties associated with the fluxes in the budget.

B1. Uncertainty in the C_{ant} Calculations

[54] The TTD method contains several assumptions that give rise to uncertainties of various magnitudes. These include assumption of the Δ/Γ value, the CFC surface saturation, analytical errors of the CFC, uncertainties in the surface water history of the used tracer, the empirical relationship for preformed TA, and the dissociation constants for the carbonate system. From these uncertainties *Waugh et al.* [2006] estimated an uncertainty of ±6 μmol kg^{-1} for individual C_{ant} estimates, and *Tanhua et al.* [2008] estimated an uncertainty in the C_{ant} derived using the TTD method of ~10%. In addition to the above mentioned uncertainties there are other assumptions in the TTD approach that are not accounted for, e.g., steady state transport and the assumption of a single dominant water mass source [*Waugh et al.*, 2006]. Especially the latter might give a relatively large uncertainty in the Nordic Seas due to mixing between recently ventilated waters (e.g., AW or Arctic Intermediate Water) and older deep waters formed in the Nordic Seas or the Arctic Ocean [e.g., *Turrell et al.*, 1999; *Rudels et al.,* 2005]. *Olsen et al.* [2010] recently estimated the uncertainties in TTD-based C_{ant} estimates in the Nordic Seas. They concluded that changes in Δ/Γ of ±0.5 (from unity) generally had a relatively small effect (less than 1 μmol kg^{-1}), but a maximum increase of the deep-water values of ~4 μmol kg^{-1} was observed when the ratio was decreased from 1 to 0.5. A potentially large error is connected with the assumption that the CO_2 disequilibrium has remained constant through time, and time evolving CO_2 disequilibrium translate essentially linearly into the C_{ant} estimates; assuming a surface water CO_2 growth rate corresponding to 80% of the atmospheric growth rate gives a decrease in estimated C_{ant} of 20%.

[55] To assess the uncertainties in the TTD-derived C_{ant} concentrations we propagated the method-based uncertainty of ±6 μmol kg^{-1} [*Waugh et al.*, 2006] and the standard error ($\sigma/\sqrt{n}$; where σ is the standard deviation (Table 2) and n is the sample size) of the C_{ant} mean values. For the NCC, ice, and runoff we applied an uncertainty of 10%.

B2. Propagation of Errors in the Carbon Budget

[56] In order to estimate the uncertainties in the budget we propagated the errors included in the transport calculations. We included observed variability in the respective volume transports both for the individual advective sources and sinks and the net fluxes. The errors in the advective transport of DIC and DOC (σ_{DIC} and σ_{DOC}, respectively) were computed by assuming that errors in ρ were negligible so that the error associated with the transport, T (corresponding to the first term in equation (1)), was calculated from:

$$\sigma_T = \rho \times \sigma_{VC} \tag{B1}$$

where σ_{VC} is given by

$$\sigma_{VC}^2 = \{C \times \sigma_V\}^2 + \{V \times \sigma_C\}^2 \tag{B2}$$

Here σ_V is the observed variability in the individual volume transports (see section 4.1), and σ_C is the standard deviation in the mean concentration of DIC or DOC (see Table 2); the σ_C values for DIC in the different water masses were in the range 0.1–1.6%, which is well above the analytical uncertainty of <0.05% [e.g., *Johnson et al.*, 1987]. The standard deviation in the mean DOC values was between 4 and 12%, which is clearly higher than the analytical uncertainty for DOC of approximately 2% [e.g., *Amon et al.*, 2003]. For the ice import in Fram Strait we adopted the estimated DOC uncertainty from *Anderson et al.* [1998] of 40%.

[57] The uncertainties in the carbon concentrations of all advective sinks and sources are found in Table 2. The errors in the burial of POC and carbonate are estimated from the cited studies described in section 4.2; *Berner* [1982] for POC, and *Milliman* [1993] for carbonate. The error in the storage is associated with uncertainties in the TTD method [*Olsen et al.*, 2010] (see section 4.3).

B3. Budget Uncertainty Under the Constraint of Mass Conservation

[58] The surface area of the Nordic Seas is about $3{\cdot}10^6$ km^2. This implies that a 0.1 Sv imbalance in the volume budget – about 1% of the total inflow – corresponds to a mean sea level rise of more than 1 m per year, which is unrealizable (see also *Hansen and Østerhus* [2007] for a similar argument). The Nordic Seas' variable exchange of water masses with the ambient oceans can therefore for the present purpose be considered constrained by the conservation of mass:

$$\sum \rho_i V_i = 0, \text{ and } \sum \rho_i v_i = 0, \tag{B3}$$

where ρ_i, V_i and v_i, respectively, are the density, mean and variable volume transports of DS, IFR, FSC, BSO, and FS exchanges. The corresponding carbon concentration (e.g., DIC) of water mass i is

$$C_i = C_0 + \Delta C_i + c_i, \tag{B4}$$

where ΔC_i is the anomalous concentration relative to a reference mean concentration C_0 (which under the constraint of mass balance does not contribute to the net carbon budget), and c_i is the associated observational uncertainty. The appropriate reference for the present case is C_0 = 2132 μmol kg^{-1}, the volume transport-weighted DIC mean from the combined total in- and outflow transports of Tables 1 and 2. The approach is equivalent to the consistent constraining of ocean heat or salt budgets [e.g., *Schauer and Beszczynska-Möller*, 2009].

[59] The net advective carbon budget for the Nordic Seas taking into account variable mass transports of the individual branches is thus

$$\sum \rho_i (V_i + v_i)(\Delta C_i + c_i) = \sum \rho_i V_i \Delta C_i + \sum \rho_i v_i \Delta C_i + \sum \rho_i V_i c_i + \sum \rho_i v_i c_i, \tag{B5}$$

when using the constraint of total mass conservation (B3). The first term on the right hand side, $\sum \rho_i V_i \Delta C_i$, is the estimated mean advective carbon budget (cf. section 5.2), and the last term on the right hand side can be neglected assuming that the variable mass transports are uncorrelated with the concentration uncertainties (or simply from the expectation that it will be dominated by the preceding term, the error associated with uncertain carbon concentrations alone that was estimated to be 0.06 Gt C yr^{-1} in section 6). The error associated with variable exchanges is therefore

$$e = |\sum \rho_i v_i \Delta C_i|, \tag{B6}$$

or

$$0 \le e \le \sum \rho_i |v_i| |\Delta C_i|. \tag{B7}$$

The right hand side of equation (B7) can be estimated from the DIC concentrations of Table 2 (less C_0), and the densities and variable volume transports given in Tables 1 and 2. The result is

$$0 \le e \le 0.06 \text{ Gt C yr}^{-1}.$$

An upper estimate of the uncertainty associated with variable or uncertain volume transports is thus that it contributes equally with the uncertainty from individual carbon concentrations to that of the total budget. It should be noted that neither the above nor the total budget explicitly takes into account any eddy exchange across the gateways to the Nordic Seas; a regional quantification of its importance does not exist to our knowledge. It has, however, been inferred to be relatively negligible compared to advection for the main gateway, the Greenland-Scotland Ridge [*Hansen and Østerhus*, 2000].

[60] **Acknowledgments.** This research was supported by the Norwegian Research Council through the projects CARBON-HEAT, A-CARB, and IPY-BIAC, and from EU IP CARBOOCEAN and the FP7 projects CarboChange (project reference 264879) and EURO-BASIN (264933). We acknowledge the three anonymous reviewers; their comments lead to several improvements to the manuscript. This is publication A370 from the Bjerknes Centre for Climate Research.

References

Aagaard, K., and E. Carmack (1989), The role of sea ice and other fresh water in the Arctic circulation, *J. Geophys. Res.*, *94*, 14,485–14,498.

Aksenov, Y., S. Bacon, A. C. Coward, and A. J. G. Nurser (2010), The North Atlantic inflow to the Arctic Ocean: High-resolution model study, *J. Mar. Syst.*, *79*(1–2), 1–22, doi:10.1016/j.jmarsys.2009.05.003.

Amon, R. M. W., G. Budéus, and B. Meon (2003), Dissolved organic carbon distribution and origin in the Nordic Seas: Exchanges with the Arctic Ocean and the North Atlantic, *J. Geophys. Res.*, *108*(C7), 3221, doi:10.1029/2002JC001594.

Anderson, L. G., K. Olsson, and M. Chierici (1998), A carbon budget for the Arctic Ocean, *Global Biogeochem. Cycles*, *12*(3), 455–465, doi:10.1029/98GB01372.

Arrigo, K. R., S. Pabi, G. L. van Dijken, and W. Maslowski (2010), Air-sea flux of CO_2 in the Arctic Ocean, 1998–2003, *J. Geophys. Res.*, *115*, G04024, doi:10.1029/2009JG001224.

Bauerfeind, E., E.-M. Nöthig, A. Beszczynska, K. Fahl, L. Kaleschke, K. Kreker, M. Klages, T. Soltwedel, C. Lorenzen, and J. Wegner (2009), Particle sedimentation patterns in the eastern Fram Strait during 2000–2005: Results from the Arctic long-term observatory HAUSGARTEN, *Deep Sea Res., Part I*, *56*(9), 1471–1487, doi:10.1016/j.dsr.2009.04.011.

Bellerby, R. G. J., A. Olsen, T. Furevik, and L. G. Anderson (2005), Response of the surface ocean CO_2 system in the Nordic Seas and the Northern North Atlantic to climate change, in *The Nordic Seas: An Integrated Perspective*, *Geophys. Monogr. Ser.*, vol. 158, edited by H. Drange et al., pp. 189–198, AGU, Washington, D. C.

Benner, R., P. Louchouarn, and R. M. W. Amon (2005), Terrigenous dissolved organic matter in the Arctic Ocean and its transport to surface and deep waters of the North Atlantic, *Global Biogeochem. Cycles*, *19*, GB2025, doi:10.1029/2004GB002398.

Bergström, S., and B. Carlsson (1994), River runoff to the Baltic Sea: 1950–1990, *Ambio*, *23*(4–5), 280–287.

Berner, R. A. (1982), Burial of organic carbon and pyrite sulfur in the modern ocean; its geochemical and environmental significance, *Am. J. Sci.*, *282*(4), 451–473, doi:10.2475/ajs.282.4.451.

Björk, G., B. G. Gustafsson, and A. Stigebrandt (2001), Upper layer circulation of the Nordic seas as inferred from the spatial distribution of heat and freshwater content and potential energy, *Polar Res.*, *20*(2), 161–168, doi:10.1111/j.1751-8369.2001.tb00052.x.

Blindheim, J. (1989), Cascading of Barents Sea bottom water into the Norwegian Sea, *Rapp. P. V. Reun. Cons. Int. Explor. Mer*, *188*, 49–58.

Blindheim, J., and F. Rey (2004), Water-mass formation and distribution in the Nordic Seas during the 1990s, *ICES J. Mar. Sci.*, *61*(5), 846–863, doi:10.1016/j.icesjms.2004.05.003.

Blindheim, J., V. Borovkov, B. Hansen, S.-A. Malmberg, W. R. Turrell, and S. Østerhus (2000), Upper layer cooling and freshening in the Norwegian Sea in relation to atmospheric forcing, *Deep Sea Res.*, *47*(4), 655–680, doi:10.1016/S0967-0637(99)00070-9.

Børsheim, K. Y., S. M. Myklestad, and J.-A. Sneli (1999), Monthly profiles of DOC, mono- and polysaccharides at two locations in the Trondheimsfjord (Norway) during two years, *Mar. Chem.*, *63*(3–4), 255–272, doi:10.1016/S0304-4203(98)00066-8.

Cisewski, B., G. Budéus, and G. Krause (2003), Absolute transport estimates of total and individual water masses in the northern Greenland Sea derived from hydrographic and acoustic Doppler current profiler measurements, *J. Geophys. Res.*, *108*(C9), 3298, doi:10.1029/2002JC001530.

Dickson, A. G., and F. J. Millero (1987), A comparison of the equilibrium constants for the dissociation of carbonic acid in seawater media, *Deep Sea Res.*, *34*, 1733–1743, doi:10.1016/0198-0149(87)90021-5.

Dickson, R. R., and J. Brown (1994), The production of North Atlantic Deep Water: Sources, rates, and pathways, *J. Geophys. Res.*, *99*(C6), 12,319–12,341, doi:10.1029/94JC00530.

Dickson, R., B. Rudels, S. Dye, M. Karcher, J. Meincke, and I. Yashayaev (2007), Current estimates of freshwater flux through Arctic and subarctic seas, *Prog. Oceanogr.*, *73*(3–4), 210–230, doi:10.1016/j.pocean.2006.12.003.

Eldevik, T., F. Straneo, A. B. Sandø, and T. Furevik (2005), Pathways and export of Greenland Sea water, in *The Nordic Seas: An Integrated Perspective*, *Geophys. Monogr. Ser.*, vol. 158, edited by H. Drange et al., pp. 89–103, AGU, Washington, D. C.

Eldevik, T., J. E. Ø. Nilsen, D. Iovino, K. A. Olsson, A. B. Sandø, and H. Drange (2009), Observed sources and variability of Nordic seas overflow, *Nat. Geosci.*, *2*, 406–410, doi:10.1038/ngeo518.

Fahrbach, E., J. Meincke, S. Østerhus, G. Rohardt, U. Schauer, V. Tverberg, and J. Verduin (2001), Direct measurements of volume transports through Fram Strait, *Polar Res.*, *20*(2), 217–224, doi:10.1111/j.1751-8369.2001.tb00059.x.

Gammelsrød, T., and B. Hackett (1981), The circulation of the Skagerrak determined by inverse methods, in *The Norwegian Coastal Current, Proceedings from the Norwegian Coastal Current Symposium*, *Geilo, 9–12 Sept, 1980*, vol. 1, edited by R. Sætre and M. Mork, pp. 311–330, Univ. of Bergen, Bergen, Norway.

Gammon, R., J. Cline, and D. Wisegarver (1982), Chlorofluoromethanes in the northeast Pacific Ocean: Measured vertical distributions and application as transient tracers of upper ocean mixing, *J. Geophys. Res.*, *87*(C12), 9441–9454, doi:10.1029/JC087iC12p09441.

Gascard, J.-C., G. Raisbeck, S. Sequeira, F. Yiou, and K. A. Mork (2004), The Norwegian Atlantic Current in the Lofoten basin inferred from hydrological and tracer data (129I) and its interaction with the Norwegian Coastal Current, *Geophys. Res. Lett.*, *31*, L01308, doi:10.1029/2003GL018303.

Gruber, N., C. D. Keeling, and N. R. Bates (2002), Interannual variability in the North Atlantic Ocean carbon sink, *Science*, *298*(5602), 2374–2378, doi:10.1126/science.1077077.

Gruber, N., et al. (2009), Oceanic sources, sinks, and transport of atmospheric CO_2, *Global Biogeochem. Cycles*, *23*, GB1005, doi:10.1029/2008GB003349.

Hall, T. M., T. W. N. Haine, and D. W. Waugh (2002), Inferring the concentration of anthropogenic carbon in the ocean from tracers, *Global Biogeochem. Cycles*, *16*(4), 1131, doi:10.1029/2001GB001835.

Hansen, B., and S. Østerhus (2000), North Atlantic–Nordic Seas exchanges, *Prog. Oceanogr.*, *45*(2), 109–208, doi:10.1016/S0079-6611(99)00052-X.

Hansen, B., and S. Østerhus (2007), Faroe Bank Channel overflow 1995–2005, *Prog. Oceanogr.*, *75*(4), 817–856, doi:10.1016/j.pocean.2007.09.004.

Hansen, B., S. Østerhus, H. Hatun, R. Kristiansen, and K. M. H. Larsen (2003), The Iceland-Faroe inflow of Atlantic water to the Nordic Seas, *Prog. Oceanogr.*, *59*(4), 443–474, doi:10.1016/j.pocean.2003.10.003.

Hansen, B., S. Østerhus, W. R. Turrell, S. Jónsson, H. Valdimarsson, H. Hátún, and S. M. Olsen (2008), The inflow of Atlantic Water, heat, and salt to the Nordic Seas across the Greenland-Scotland Ridge, in *Arctic-Subarctic Ocean Fluxes: Defining the Role of the Northern Seas in Climate*, edited by R. R. Dickson, J. Meincke, and P. Rhines, pp. 15–43, Springer, Dordrecht, Netherlands.

Herbaut, C., and M.-N. Houssais (2009), Response of the eastern North Atlantic subpolar gyre to the North Atlantic Oscillation, *Geophys. Res. Lett.*, *36*, L17607, doi:10.1029/2009GL039090.

Hjalmarsson, S., K. Wesslander, L. G. Anderson, A. Omstedt, M. Perttilä, and L. Mintrop (2008), Distribution, long-term development and mass balance calculation of total alkalinity in the Baltic Sea, *Cont. Shelf Res.*, *28*, 593–601, doi:10.1016/j.csr.2007.11.010.

Hjalmarsson, S., L. G. Anderson, and J. She (2010), The exchange of dissolved inorganic carbon between the Baltic Sea and the North Sea in 2006 based on measured data and water transport estimates from a 3D model, *Mar. Chem.*, *121*, 200–205, doi:10.1016/j.marchem.2010.04.008.

Ingvaldsen, R. B., L. Asplin, and H. Loeng (2004), The seasonal cycle in the Atlantic transport to the Barents Sea during the years 1997–2001, *Cont. Shelf Res.*, *24*(9), 1015–1032, doi:10.1016/j.csr.2004.02.011.

Jahnke, R. A. (1996), The global ocean flux of particulate organic carbon: Areal distribution and magnitude, *Global Biogeochem. Cycles*, *10*(1), 71–88, doi:10.1029/95GB03525.

Jakobsson, M. (2002), Hypsometry and volume of the Arctic Ocean and its constituent seas, *Geochem. Geophys. Geosyst.*, *3*(5), 1028, doi:10.1029/2001GC000302.

Jeansson, E. (2005), Chemical tracers in the Nordic Seas: Studies on water masses and anthropogenic carbon, Ph.D. thesis, Göteborg Univ., Göteborg, Sweden.

Jeansson, E., S. Jutterström, B. Rudels, L. G. Anderson, K. A. Olsson, E. P. Jones, W. M. Smethie Jr., and J. H. Swift (2008), Sources to the East Greenland Current and its contribution to the Denmark Strait Overflow, *Prog. Oceanogr.*, *78*, 12–28, doi:10.1016/j.pocean.2007.08.031.

Jeansson, E., K. A. Olsson, T. Tanhua, and J. L. Bullister (2010), Nordic Seas and Arctic Ocean CFC data in CARINA, *Earth Syst. Sci. Data*, *2*, 79–97, doi:10.5194/essd-2-79-2010.

Johnson, K. M., J. M. Sieburth, P. J. l. Williams, and L. Brändström (1987), Coulometric total carbon dioxide analysis for marine studies: Automation and calibration, *Mar. Chem.*, *21*(2), 117–133, doi:10.1016/0304-4203(87)90033-8.

Jónsson, S., and H. Valdimarsson (2005), The flow of Atlantic water to the North Icelandic Shelf and its relation to the drift of cod larvae, *ICES J. Mar. Sci.*, *62*(7), 1350–1359, doi:10.1016/j.icesjms.2005.05.003.

Jutterström, S., and L. G. Anderson (2010), Uptake of CO_2 by the Arctic Ocean in a changing climate, *Mar. Chem.*, *122*, 96–104, doi:10.1016/j.marchem.2010.07.002.

Jutterström, S., and E. Jeansson (2008), Anthropogenic carbon in the East Greenland Current, *Prog. Oceanogr.*, *78*, 29–36, doi:10.1016/j.pocean.2008.04.001.

Jutterström, S., E. Jeansson, L. G. Anderson, R. Bellerby, E. P. Jones, W. M. Smethie Jr., and J. H. Swift (2008), Evaluation of anthropogenic carbon in the Nordic Seas using observed relationships of N, P and C versus CFCs, *Prog. Oceanogr.*, *78*, 78–84, doi:10.1016/j.pocean.2007.06.001.

Key, R. M., et al. (2010), The CARINA data synthesis project: Introduction and overview, *Earth Syst. Sci. Data*, *2*, 105–121, doi:10.5194/essd-2-105-2010.

Kivimäe, C., R. G. J. Bellerby, A. Fransson, M. Reigstad, and T. Johannessen (2010), A carbon budget for the Barents Sea, *Deep Sea Res., Part I*, *57*, 1532–1542, doi:10.1016/j.dsr.2010.05.006.

Lewis, E., and D. W. R. Wallace (1998), Program developed for CO_2 system calculations, Rep. ORNL/CDIAC-105, Carbon Dioxide Inf. Anal. Cent., Oak Ridge Natl. Lab., U.S. Dep. of Energy, Oak Ridge, Tenn.

Lundberg, L., and P. M. Haugan (1996), A Nordic Seas–Arctic Ocean carbon budget from volume flows and inorganic carbon data, *Global Biogeochem. Cycles*, *10*(3), 493–510, doi:10.1029/96GB00359.

Macrander, A., U. Send, H. Valdimarsson, S. Jónsson, and R. H. Käse (2005), Interannual changes in the overflow from the Nordic Seas into the Atlantic Ocean through Denmark Strait, *Geophys. Res. Lett.*, *32*, L06606, doi:10.1029/2004GL021463.

Mauritzen, C. (1996), Production of dense overflow waters feeding the North Atlantic across the Greenland-Scotland Ridge. Part 1: Evidence for a revised circulation scheme, *Deep Sea Res., Part I*, *43*(6), 769–806, doi:10.1016/0967-0637(96)00037-4.

Mehrbach, C., C. H. Culberson, J. E. Hawlay, and R. M. Pytkowicz (1973), Measurements of the apparent dissociation constants of carbonic acid in seawater at atmospheric pressure, *Limnol. Oceanogr.*, *18*, 897–907, doi:10.4319/lo.1973.18.6.0897.

Millero, F. J. (1979), The thermodynamics of the carbonate system in seawater at atmospheric pressure, *Geochim. Cosmochim. Acta*, *43*, 1651–1661.

Milliman, J. D. (1993), Production and accumulation of calcium carbonate in the ocean: Budget of a nonsteady state, *Global Biogeochem. Cycles*, *7*(4), 927–957, doi:10.1029/93GB02524.

Nilsen, J. E. Ø., and E. Falck (2006), Variations of mixed layer properties in the Norwegian Sea for the period 1948–1999, *Prog. Oceanogr.*, *70*(1), 58–90, doi:10.1016/j.pocean.2006.03.014.

Nilsson, J., G. Björk, B. Rudels, P. Winsor, and D. Torres (2008), Liquid freshwater transport and Polar Surface Water characteristics in the East Greenland Current during the AO-02 Oden expedition, *Prog. Oceanogr.*, *78*(1), 45–57, doi:10.1016/j.pocean.2007.06.002.

Nondal, G., R. G. J. Bellerby, A. Olsen, T. Johannessen, and J. Olafsson (2009), Optimal evaluation of the surface ocean CO_2 system in the northern North Atlantic using data from voluntary observing ships, *Limnol. Oceanogr. Methods*, *7*, 109–118, doi:10.4319/lom.2009.7.109.

Olsen, A. (2009a), Nordic Seas total dissolved inorganic carbon data in CARINA, *Earth Syst. Sci. Data*, *1*, 35–43, doi:10.5194/essd-1-35-2009.

Olsen, A. (2009b), Nordic Seas total alkalinity data in CARINA, *Earth Syst. Sci. Data*, *1*, 77–86, doi:10.5194/essd-1-77-2009.

Olsen, A., R. G. J. Bellerby, T. Johannessen, A. M. Omar, and I. Skjelvan (2003), Interannual variability in the wintertime air-sea flux of carbon dioxide in the northern North Atlantic, 1981–2001, *Deep Sea Res., Part I*, *50*(10–11), 1323–1338, doi:10.1016/S0967-0637(03)00144-4.

Olsen, A., et al. (2006), Magnitude and origin of the anthropogenic CO_2 increase and ^{13}C Suess effect in the Nordic seas since 1981, *Global Biogeochem. Cycles*, *20*, GB3027, doi:10.1029/2005GB002669.

Olsen, A., et al. (2009), Overview of the Nordic Seas CARINA data and salinity measurements, *Earth Syst. Sci. Data*, *1*, 25–34, doi:10.5194/essd-1-25-2009.

Olsen, A., A. M. Omar, E. Jeansson, L. G. Anderson, and R. G. J. Bellerby (2010), Nordic Seas transit-time distributions and anthropogenic CO_2, *J. Geophys. Res.*, *115*, C05005, doi:10.1029/2009JC005488.

Østerhus, S., W. R. Turrell, S. Jónsson, and B. Hansen (2005), Measured volume, heat, and salt fluxes from Atlantic to the Arctic Mediterranean, *Geophys. Res. Lett.*, *32*, L07603, doi:10.1029/2004GL022188.

Pérez, F. F., M. Vázquez-Rodríguez, H. Mercier, A. Velo, P. Lherminier, and A. F. Ríos (2010), Trends of anthropogenic CO_2 storage in North Atlantic water masses, *Biogeosciences*, *7*, 1789–1807, doi:10.5194/bg-7-1789-2010.

Quadfasel, D., and R. Käse (2007), Present-day manifestation of the Nordic Seas overflows, in *Ocean Circulation: Mechanisms and Impacts*, *Geophys. Monogr. Ser.*, vol. 173, edited by A. Schmittner, J. C. H. Chiang, and S. Hemming, pp. 75–90, AGU, Washington, D. C.

Rudels, B. (1987), On the mass balance of the Polar Ocean, with special emphasis on the Fram Strait, *Norsk Polarinst. Skrifter*, *188*, 53 pp.

Rudels, B., H. J. Friedrich, and D. Quadfasel (1999), The Arctic Circumpolar Boundary Current, *Deep Sea Res., Part II*, *46*(6–7), 1023–1062, doi:10.1016/S0967-0645(99)00015-6.

Rudels, B., R. Meyer, E. Fahrbach, V. V. Ivanov, S. Østerhus, D. Quadfasel, U. Schauer, V. Tverberg, and R. A. Woodgate (2000), Water mass distribution in Fram Strait and over the Yermak Plateau in summer 1997, *Ann. Geophys.*, *18*(6), 687–705, doi:10.1007/s00585-000-0687-5.

Rudels, B., G. Björk, J. Nilsson, P. Winsor, I. Lake, and C. Nohr (2005), The interaction between waters from the Arctic Ocean and the Nordic Seas north of Fram Strait and along the East Greenland Current: Results from the Arctic Ocean-02 Oden expedition, *J. Mar. Syst.*, *55*(1–2), 1–30, doi:10.1016/j.jmarsys.2004.06.008.

Sabine, C. L., et al. (2004), The oceanic sink for anthropogenic CO_2, *Science*, *305*, 367–371, doi:10.1126/science.1097403.

Sarmiento, J. L., and N. Gruber (2002), Sinks for anthropogenic carbon, *Phys. Today*, *55*(8), 30–36, doi:10.1063/1.1510279.

Sarmiento, J. L., P. Monfray, E. Maier-Reimer, O. Aumont, R. J. Murnane, and J. C. Orr (2000), Sea-air CO_2 fluxes and carbon transport: A comparison of three ocean general circulation models, *Global Biogeochem. Cycles*, *14*(4), 1267–1281, doi:10.1029/1999GB900062.

Saunders, P. M. (1990), Cold outflow from the Faroe Bank Channel, *J. Phys. Oceanogr.*, *20*, 29–43, doi:10.1175/1520-0485(1990)020<0029:COFTFB>2.0.CO;2.

Saunders, P. M. (1996), The flux of dense cold overflow water southeast of Iceland, *J. Phys. Oceanogr.*, *26*, 85–95, doi:10.1175/1520-0485(1996)026<0085:TFODCO>2.0.CO;2.

Schauer, U., and A. Beszczynska-Möller (2009), Problems with estimation and interpretation of oceanic heat transport—Conceptual remarks for the case of Fram Strait in the Arctic Ocean, *Ocean Sci.*, *5*, 487–494, doi:10.5194/os-5-487-2009.

Schauer, U., E. Fahrbach, S. Østerhus, and G. Rohardt (2004), Arctic warming through the Fram Strait: Oceanic heat transport from 3 years of measurements, *J. Geophys. Res.*, *109*, C06026, doi:10.1029/2003JC001823.

Schlüter, M., E. J. Sauter, A. Schäfer, and W. Ritzrau (2000), Spatial budget of organic carbon flux to the seafloor of the northern North Atlantic (60°N–80°N), *Global Biogeochem. Cycles*, *14*, 329–340, doi:10.1029/1999GB900043.

Schneider, B., G. Nausch, K. Nagel, and N. Wasmund (2003), The surface water CO_2 budget for the Baltic Proper: A new way to determine nitrogen fixation, *J. Mar. Syst.*, *42*(1–2), 53–64, doi:10.1016/S0924-7963(03)00064-2.

Schuster, U., A. J. Watson, N. R. Bates, A. Corbiere, M. Gonzalez-Davila, N. Metzl, D. Pierrot, and M. Santana-Casiano (2009), Trends in North Atlantic sea-surface fCO_2 from 1990 to 2006, *Deep Sea Res., Part II*, *56*(8–10), 620–629, doi:10.1016/j.dsr2.2008.12.011.

Skagseth, Ø. (2008), Recirculation of Atlantic Water in the western Barents Sea, *Geophys. Res. Lett.*, *35*, L11606, doi:10.1029/2008GL033785.

Skagseth, Ø., K. F. Drinkwater, and E. Terrile (2011), Wind- and buoyancy-induced transport of the Norwegian Coastal Current in the Barents Sea, *J. Geophys. Res.*, *116*, C08007, doi:10.1029/2011JC006996.

Skjelvan, I., et al. (2005), A review of the inorganic carbon cycle of the Nordic Seas and the Barents Sea, in *The Nordic Seas: An Integrated Perspective*, *Geophys. Monogr. Ser.*, vol. 158, edited by H. Drange et al., pp. 157–175, AGU, Washington, D. C.

Smedsrud, L. H., R. Ingvaldsen, J. E. Ø. Nilsen, and Ø. Skagseth (2010), Heat in the Barents Sea: Transport, storage, and surface fluxes, *Ocean Sci.*, *6*, 219–234, doi:10.5194/os-6-219-2010.

Sutherland, D. A., and R. S. Pickart (2008), The East Greenland Coastal Current: Structure, variability, and forcing, *Prog. Oceanogr.*, *78*, 58–77, doi:10.1016/j.pocean.2007.09.006.

Takahashi, T., et al. (2009), Climatological mean and decadal change in surface ocean pCO_2, and net sea-air CO_2 flux over the global oceans, *Deep Sea Res., Part II*, *56*(8–10), 554–577, doi:10.1016/j.dsr2.2008.12.009.

Tanhua, T., A. Körtzinger, K. Friis, D. W. Waugh, and D. W. R. Wallace (2007), An estimate of anthropogenic CO_2 inventory from decadal changes in oceanic carbon content, *Proc. Natl. Acad. Sci. U. S. A.*, *104*(9), 3037–3042, doi:10.1073/pnas.0606574104.

Tanhua, T., D. W. Waugh, and D. W. R. Wallace (2008), Use of SF_6 to estimate anthropogenic CO_2 in the upper ocean, *J. Geophys. Res.*, *113*, C04037, doi:10.1029/2007JC004416.

Tanhua, T., E. P. Jones, E. Jeansson, S. Jutterström, W. M. Smethie Jr., D. W. R. Wallace, and L. G. Anderson (2009), Ventilation of the Arctic Ocean: Mean ages and inventories of anthropogenic CO_2 and CFC-11, *J. Geophys. Res.*, *114*, C01002, doi:10.1029/2008JC004868.

Tanhua, T., S. van Heuven, R. M. Key, A. Velo, A. Olsen, and C. Schirnick (2010), Quality control procedures and methods of the CARINA database, *Earth Syst. Sci. Data*, *2*, 35–49, doi:10.5194/essd-2-35-2010.

Thomas, H., Y. Bozec, H. J. W. De Baar, K. Elkalay, M. Frankignoulle, L.-S. Schiettecatte, G. Kattner, and A. Borges (2005), The carbon budget of the North Sea, *Biogeosciences*, *2*, 87–96, doi:10.5194/bg-2-87-2005.

Thomas, H., A. E. F. Prowe, I. D. Lima, S. C. Doney, R. Wanninkhof, R. J. Greatbatch, U. Schuster, and A. Corbière (2008), Changes in the North Atlantic Oscillation influence CO_2 uptake in the North Atlantic over the past 2 decades, *Global Biogeochem. Cycles*, *22*, GB4027, doi:10.1029/2007GB003167.

Turrell, W. R., G. Slesser, R. D. Adams, R. Payne, and P. A. Gillibrand (1999), Decadal variability in the composition of Faroe Shetland Channel bottom water, *Deep Sea Res., Part I*, *46*(1), 1–25, doi:10.1016/S0967-0637(98)00067-3.

Ullman, D. J., G. A. McKinley, V. Bennington, and S. Dutkiewicz (2009), Trends in the North Atlantic carbon sink: 1992–2006, *Global Biogeochem. Cycles*, *23*, GB4011, doi:10.1029/2008GB003383.

Vinje, T. (2001), Fram Strait ice fluxes and atmospheric circulation: 1950–2000, *J. Clim.*, *14*(16), 3508–3517, doi:10.1175/1520-0442(2001)014<3508:FSIFAA>2.0.CO;2.

Watson, A. J., et al. (2009), Tracking the variable North Atlantic sink for atmospheric CO_2, *Science*, *326*(5958), 1391–1393, doi:10.1126/science.1177394.

Waugh, D. W., T. W. N. Haine, and T. M. Hall (2004), Transport times and anthropogenic carbon in the subpolar North Atlantic Ocean, *Deep Sea Res., Part I*, *51*(11), 1475–1491.

Waugh, D. W., T. M. Hall, B. I. McNeil, R. Key, and R. J. Matear (2006), Anthropogenic CO_2 in the oceans estimated using transit time distributions, *Tellus, Ser. B*, *58*, 376–389.

Wheeler, P. A., M. Gosselin, E. Sherr, D. Thibaultc, D. L. Kirchman, R. Benner, and T. E. Whitledge (1996), Active cycling of organic carbon in the central Arctic Ocean, *Nature*, *380*(6576), 697–699, doi:10.1038/380697a0.

Wheeler, P. A., J. M. Watkins, and R. L. Hansing (1997), Nutrients, organic carbon and organic nitrogen in the upper water column of the Arctic Ocean: Implications for the sources of dissolved organic carbon, *Deep Sea Res., Part II*, *44*(8), 1571–1592, doi:10.1016/S0967-0645(97)00051-9.

R. G. J. Bellerby, E. Jeansson, A. M. Omar, and I. Skjelvan, Uni Bjerknes Centre, Uni Research AS, Allégaten 55, NO-5007 Bergen, Norway. (emil.jeansson@uni.no)

T. Eldevik and E. Falck, Geophysical Institute, University of Bergen, Allégaten 70, NO-5007 Bergen, Norway.

T. Johannessen and S. K. Lauvset, Bjerknes Centre for Climate Research, Allégaten 55, NO-5007 Bergen, Norway.

J. E. Ø. Nilsen, Nansen Environmental and Remote Sensing Centre, Thormøhlensgate 47, NO-5006 Bergen, Norway.

A. Olsen, Institute for Marine Research, PO Box 1870 Nordnes, NO-5817 Bergen, Norway.